

12

**Final Report: Air Sea Interaction Processes Associated with
Gulf Stream Frontal Features**

Contract: N00014-91-K-2030

PI: John M. Morrison

Institution: North Carolina State University

Date: 20 May 1992

**DTIC
ELECTE
S DEC 20 1993
A**

INTRODUCTION

This document reports on the research associated with Contract N0014-91-K-2030 with the Naval Research Laboratory, Center for Space Sensing. We have been working closely with Dr. Farid Askari (Code 2020). As outlined in the original proposal, this work is focusing on : the Real Aperture Radar (RAR), Scatterometer, and Laser Profilometer measurements made during October 1990 in the vicinity of the Gulf Stream. While data reduction effort have focused on RAR imaging of oceanic fronts with particular emphasis on radar reasurements collected at low grazing incidence. RAR measurements were made on three days during the course of the study. This report focuses on the data collected on 3 October 1990.

Data for this project were collected between 1 - 5 October 1990 during a joint air-sea interaction study between the Department of Marine, Earth and Atmospheric Sciences, North Carolina State University and the Naval Research Laboratory. The study was located offshore of North Carolina in the southern portion of the Middle Atlantic Bight in the vicinity of the Gulf Stream. The study involved both airborne and shipboard activities.

Airborne activities focused on remotely sensed measurements of the sea surface in the region of the Gulf Stream front and observations of artifical sea slicks. Remotely sensed data were collected aboard the NRL-P3 by Dr. Farid Askari and included Ku-band scatterometer, laser profilometer, PRT-5 precision radiometer, and RAR measurements taken at X-band.

Shipboard measurements were collected on the R/V Cape Hatteran under the supervision of Drs. John Morrison and Sethu Raman. A variety of measurements and observations were made including: radiosonde, CTD, XBT measurements and meteorological measurements. In addition, Acoustic Doppler Current Profiler and

This document has been approved
for public release and sale; its
distribution is unlimited.

93 12 17018

AD-A273 912

93-30580

Serial Ascii Instrument Loop (SAIL) continuously collect data on sea surface temperature and salinity, air temperature, pressure, wind speed and direction. Humidity measurements were collected ever half-hour by the students.

Ancillary data included AVHRR-HRPT infrared SST images provided by the University of Miami, Rosenthal School of Marine and Atmospheric Science, SSM/I data from the Defense Meteorological Satellite Program, and C-MAN and buoy data from NODC. The data from these products provided synoptic information on the Gulf Stream and the atmospheric boundary layer within the study region.

DATA ACQUISITION

Six RAR transects were flown in the region of the Gulf Stream front between 16:00 and 18:00 gmt, on 3 October. Four ship transects normal to the Gulf Stream front were made between 11:30 and 23:00 gmt in the same area. The shipboard observations during the transects provided sea truth for the airborne remote sensing activities. Figure 1, shows the flight tracts with respect to the Gulf Stream SST front. The ship tracts, not shown for reasons of clarity, essentially fall with in the area bounded by RAR tracts 23 and 24. A brief description of the instruments used in the data acquisition is discussed, subsequently.

Shipboard Measurements

Both atmospheric and oceanographic measurements were made prior during, and after the P3 over flights. Atmospheric measurements consisted of marine deck observations of air temperature, pressure, humidity, wind speed and direction. Four minisondes were also launched between 8:00 and 19:00 gmt with two deployments on each side of the GSF. Table one lists the location and times of each minisonde deployment. Oceanographic measurements include sst and salinity, CTD, XBT, and ADCP observations. CTD measurements consisted of a one transect (7 stations) acquired approximately between 12 to 6 hours prior to the beginning of the over flights. Four ADCP transects were taken between 11:00 and 23:00 gmt, two of which where concurrent with the RAR Observations. Eleven XBTs were dropped between 17:00 and 19:00 gmt.

ADCP Measurements

The R/V Cape Hatteras is equipped with an RDI model RD-DR150, 150 kHz acoustic doppler instrument capable of profiling depths to over 300 m. The instrument was connected to the ship's pitch and roll sensors, gyroscope, and to the GPS navigation system. Data were sampled in four meter bins with one acoustical ping per second. Further processing included averaging the data in three minute time intervals. This served to smooth and reduce the data to a manageable size for cross sectional analysis with out lose of integrity.

CTD Measurements

CTD casts were acquired with a Sea-bird Instruments Conductivity-Temperature-Depth probe. Measurements were taken at a depth of 500 meters during the CTD deployments mentioned previously. Water samples were taken at depths of 10, 50, 100, 300, and 500 meters at several stations. Salinity was determined on each of these samples with a guideline Autosal Salinometer. These measurements were then used to calibrate the conductivity sensor on the CTD.

XBT Measurements

Temperature profiles were acquired with Sippicon Inc. T-4s. Thermal data are converted from frequency counts to temperature counts at the front end processor at the time of deployment. Post processing involved the conversion of bin counts to depth by applying the supplied drop parameters to the drop equation which gives a one to one correspondence between temperature and depth. Temperature counts were then converted to actual values by applying the temperature conversion equation, along with the T-4 thermal parameters to each probe. Depth vs temperature profiles were then constructed, and where applicable cross sectional plots.

Airborne Remote Sensing Measurements

RAR imagery was collected by a 9.4 GHz (X-Band) radar with a 20 kilowatt peak power, pulse length of 50 ns, precision repeat frequency of 100 Hz and an azimuthal beam width of 0.6 degrees. On 3-October a total of six RAR tracts were flown at low resolution. Tracts were flown in a star pattern at a nominal altitude of a 175 m

<input checked="checked" type="checkbox"/>
<input type="checkbox"/>
<input type="checkbox"/>
Codes

Dist	and/or Special
A-1	

DTIC QUALITY INSPECTED 1

at an air speed of 100 m/s. A typical swath width at this altitude is in the order of 2.5 km.

PRELIMINARY RESULTS

Preliminary results for 3-Oct-1990 are presented in this section. The first part of this section addresses the acquired sea truth and the following part with present some of the results of the RAR.

Sea Truth

Figure 2. depicts the synoptic sst field acquired from NOAA-11's AVHRR (channels 3 and 4) about 10 hours prior to the commencement of the remote sensing activities. (The afternoon image for 3-October was unusable because of extensive cloud cover over the region of interest). Superimposed on this image are the area wide winds as reported by buoy, C-man, and the R/V C. Hatteras at the time of the over flights. Notice that wind field is coherent between the two C-MAN stations (dsln7, chl v2) and between the buoy and the ship. However, the are approximately 90 d out of phase between the two sets. This could be a sea breeze response or due to the passage of a front, at this time it is not clear as to which. With in the study region however, winds were light, about 5 m/s, and in general, from the North-Northeast.

The sst image reveals at least the presents of three water masses, if not four, within the study area. These include: waters originating form the mid to outer shelf of the middle Atlantic bight as denoted by the blue shading in figures 1 and 2, the waters of the inner shelf of the MAB which are predominantly composed of outflow from Chesapeake and Delaware Bays, denoted by the green shading in both figures, and the waters from the Gulf Stream, denoted by the red shading. Each of these water masses has a unique temperature and salinity structure that enables a rapid determination of each type. For instance, at this time of the year (early to mid fall) inner shelf waters of the lower MAB have moderate temperatures (22-24 c) and relatively low salinity values (30-32 psu). Waters of the mid to outer shelf region, on the other hand, have converse to those of the inner shelf (18-20 c; 33-35 psu). Gulf Stream water consistently has higher temperatures and salinities then the previous two, (<35.5

psu; <27 °C) A fourth water mass of a more complex origin is also present and is associated with the GSF. The water mass has a slightly lower salinity (35 psu) and temperature (25-27) than the Gulf Stream.

The presence of these differing water masses in the study region influences RAR imaging in several ways. First, salinity can alter the emissivity of the water as can the temperature. Viscosity is modified which directly influences capillary wave production and propagation. A third influence is on the development of the marine atmospheric boundary layer which in turn modifies the development and propagation of surface waves, both capillary and gravity. A fourth influence of differing water masses in the area (though not explicitly expressed in this study) is the production of biogenic surfactants by altering the assemblages of nekton and plankton that produce these types of biochemical agents. All these effects characterize the nature of radar backscatter from the sea surface.

Shipboard survey results

Figure 3a depicts the shipboard measurements acquired during transect A. Wind speeds varied between 2 and 6 m/s with an approximate average of 4 m/s. Wind direction varied from 230 T to 180 T. The average was around 200 T. While the wind speed was consistent across the entire range of the transect, wind direction shows a general backing of the wind as the GSF is crossed. Both SST and salinity clearly illuminate the SST front of the Gulf Stream at 16 km into the tract. The current velocity at 8 m shows a general decreasing linear trend along the transect with departures from this at 8, 14, and 16 km. Current shear mimics current speed. Figure 3b illustrates the ADCP cross section, along with SST, and ship wind vectors. Again wind vectors reveal the backing and decreasing wind speed as the SST front is approached and crossed. The ADCP profile of the upper 200 m along the transect shows a rich and complex current regime. The departures in current speed mentioned in the preceding paragraph, are clearly visible. The departure at 8 km is associated with the the Gulf Stream velocity front while those at 16 and 18 km are coincident with the thermal front. Note that about 8 km separate the two fronts.

Transect B exhibits similar characteristics as A, in both

the atmospheric and hydrographic measurements (figures 4a and 4b.) The separation between the two fronts, however, has narrowed to 6 km. XBT profiles coinciding with the ADCP cross section are depicted in figure 4c. XBT station 7 shows the presents of a layer of cool shelf water, about 10 m thick, overlaying a layer of Gulf Stream water of 40 m extent. Between 70 and 110 m a band containing both waters of the inner and outer shelf are present. This station corresponds to a position between stations 4 and 5 on the ADCP transect shown in figure 4b.

Notice the similarities in the two profiles at this position. XBT Station 8 corresponds to ADCP station 11. This profile exhibits typical gulf stream characteristic in temperature but exhibits velocities in the order of 0.5 m/s these than the Gulf Stream. Values below 100 m in the XBT profile were eliminated because of spurious measurements. XBT profile 9 and 10 also exhibits similar Gulf Stream characteristics. However, section 9 lies shoreward of the velocity front as inferred from the cross sectional plot in figure 4b. XBT 9 occurs between ADCP stations 14 and 15. XBT 10 was deployed at the end of the transect.

The surface measurements of tract C are similar to those in tracts A and B; however, the transect length was considerably shorter (figures 5a and 5b). Also, the Gulf Stream velocity front was not encountered. A fortunate compensation for this lack of length is the acquisition of a fairly detail XBT survey with in the region of the thermal front. A total of 7 XBTs were deployed within a range of 5 km, beginning at ADCP station 2 and ending at station 11. The profiles are shown in figures 5c and 5d.

Figure 6a and 6b show the results of shipboard measurements acquired during transect D. Gulf Stream frontal structure and MABL characteristics are similar to the preceeding transects.

RAR Results

Figures 7a and 7b depict, respectively, the processed image and the preliminary results from RAR track 19. The image reveals an area of low backscatter over the first 25 km of the track. This is clearly illustrated in figure 7b, by the fact that the SST jump is coincident with a 4-6 db change in radar cross section at the same location. RCS modulations also increase with

respect to incidence angle. These modulations however, may be due to aircraft motion. This notion is suggested by the fluctuations in the RCS at nadir as observed in the image.

Figure 8a and 8b show the results for RAR 20. With respect to the image (figure 8a) a variety of interesting features are present. Some of these can be directly related to aircraft motion while others are not (for instance, the darkened area located between 38 and 46 km). Figure 8b, shows that SST front is displaced seaward by approximately 8 km, from the RAR profiles at 75 and 80 degrees incidence while at 85 degrees the two are coincident. Notice that peaks at 19 and 29 degrees (a result of aircraft motion) are coherent in the RAR and between the RAR and the scatterometer. This reason for this is not clear. It is hoped that future discussion with Dr. Askari will help clarify this observation.

The image for RAR track 22 is shown in figure 9a and the respective profiles are shown in figure 9b. This image is rich in composition, much of which has not been interpreted at this time. For instance, radar signature bisecting the image is most likely the SST Front. Other features include alternating bands of high and low radar return throughout the image. An anomalously high return area in the lower left portion of the image, and a wedge shape region of low return in the lower right portion of the image. Upon examination of figure 9b it appears that at least three distinct backscatter regions exist, but the origin and nature of these signatures, as of this time, have not been determined.

RAR track 23 is clearly the most interpretable image of the group. The ship track and flight track data were collected at the time thus limiting the temporal variability between the two data sets. Immediately noticeable in this image (Figure 10a) is the pronounced signature of two fronts. Examining Figure 10b it can be seen that a 20 db increase in the return occurs at the first front; then relaxes back to 36 db until the second front is reached. At the second front a 10 to 12 db increase is evident. The separation of these two peaks corresponds to the separation distance between the thermal and velocity front (refer to Figure 5b). The offset between the peaks and the PRT-5 is due to the fact that the PRT-5 is looking at nadir while the RAR is looking away from the aircraft while front itself is projected diagonally

in the image.

Figures 11a and 11b depict the information generated from RAR track 24. This image contains a significant amount of noise due to aircraft motion making interpretation quite difficult. However, a v shaped pattern similar to the one in observed in RAR 22 is apparent.

RAR track 25 is represented in Figures 12a and 12b. As with RAR 22, complex patterns are exhibited in the image. There also appears to be an offset between the PRT-5 and the peaks in the RCS profiles.

Basic statistics for each incidence angle and each tract appear in Table 1. Statistics are broken down in three categories: Entire tract, cool side and warm side of the sst front. The strongest returns occurred in RAR 19 (look direction 90 T; 60 to the mean wind) and in RAR 23 (look direction 0 T and 330 to the mean wind). The large variability in RAR 24 is a result of the aircraft motion. Several trends are noticeable in the data. First the warm side shows higher returns than cool side. This can be accounted for by the change in stability in the mabl over the two regions. The cool side being slightly stable to neutral and the warm side being unstable. The greater the instability the greater the surface roughness and therefore, more backscatter. A second trend that cannot, at the present time, is the increase in db with an increase in grazing incidence.

In summary, there appears to be a rich and complex set of conditions arising in the vicinity of the Gulf Stream Front. Some of these features can be directly attributed to the SST and velocity front, as can be seen in RAR 19 and RAR 23. Processes occurring within the MABL no doubt play a role in the character of the radar return, but to what degree especially in the light wind conditions present on 3 October. Hydrodynamic, as of yet not fully addressed, most play some role in the radar return, and finally the very nature of the RAR operating at a low region of incidence and interacting with material surfaces in the order of the RAR's operational wavelength may play a role in characterizing the RCS.

Marine Atmospheric Boundary Layer Model

This summer we plan to run a 2-dimension marine atmospheric boundary layer model using the observed sea surface temperature from October 3, 1990. The temperature data will be supplemented by the observed wind field in the vicinity of our measurements, the larger synoptic wind field for the region, the computed ocean surface fluxes and atmospheric sounding data. It is hoped that we will be able to directly compare the results of this model to the surface roughness on both sides of the Gulf Stream front in an effort to begin to understand the role that the marine atmospheric boundary layer plays in the modulation of the radar cross-section in the region of strong thermal and velocity shears.

SUMMARY OF ACTIVITIES ON SCATTERMETERY AND LASER PROFILOMETRY

With respect to the other tasks, this is what has been completed to date, and what needs to be accomplished:

Task: Ku-Band Scatterometer

Completed

- (1) processing and compression of scatterometer data
- (2) Sea truth data has been delivered to Dr. Askari
- (3) determination of derived mabl parameters (i.e. windstress, surface roughness, drag coefficient)

To be completed

- (1) execution of a MABL model for 3 October (This to be completed within the next several weeks)
- (2) Comparison between the Plant and SASS II models
- (3) Subsequent report on the findings.

Task: Laser Profilometer

Completed

- (1) Data reduction and spectra generation
- (2) Preliminary investigation of wave field

To be completed

At the present this task has been put on hold until the RAR analysis is completed.

SUMMARY

Above we have presented some of the preliminary results and question of the RAR imaging of the Gulf Stream region and its associated activities. It is anticipated that this activity will be complete no later than 31 July, 1992.

When the analysis of the RAR data is completed, we plan to continue, in collaboration with Dr. Farid Askari on the analysis of the Scatterometer and Laser Profilometer data. It is anticipated that a paper on the RAR analysis will be submitted for publication in the Journal of Geophysical Research this summer and that Mr. Timothy Donato will use these results in partial fulfillment of his requirement for a Master's of Science in Physical Oceanography at North Carolina State University.

At present, we plan to collaborate with Dr. Askari on two additional papers. First, the Scatterometer data will be used in a statistical comparison between the observed winds and model results using Plant's model and the SASS II model for wind oriented across and along the Gulf Stream front in order to analyze the behavior of these models in the presence of a strong ocean thermal front. Second, we plan to use the Laser Profilometer to obtain ocean wave spectra number and frequency in the vicinity of a strong ocean frontal region to determine the effects of the strong horizontal shears on the surface wave field.

TABLE 3.1 Data Collection Summary

Measure.	STN	Time	Latitude	Longitude	Depth
CTD	9	01:46:56	36 19.98	74 09.98	500
	10	02:44:34	36 17.96	74 12.48	500
	11	04:17:20	36 17.84	74 07.18	500
	12	05:21:47	36 16.00	74 04.63	500
	13	06:14:50	36 13.80	74 01.74	500
	14	07:28:57	36 10.68	73 57.84	500
	15	08:52:08	36 07.19	73 53.91	500
	16	10:01:37	36 03.38	73 49.68	500
XBT	7	16:48:05	36 21.10	74 05.62	500
	8	17:01:08	36 19.53	74 03.75	475
	9	17:15:48	36 17.84	74 01.25	500
	10	17:31:26	36 16.30	73 58.90	500
	11	18:46:36	36 19.39	74 00.98	500
	12	18:50:56	36 20.34	74 02.16	500
	13	18:54:23	36 20.76	74 02.70	500
	14	18:56:40	36 20.94	74 02.94	500
	15	19:00:03	36 21.24	74 03.30	500
	16	19:02:36	36 21.60	74 03.78	500
	17	19:04:23	36 21.78	74 04.02	500
Mini Sondes	1	11:32	36 10.44	73 56.46	500
	2	12:26	36 14.46	74 01.86	500
	3	14:25	36 21.54	74 10.62	500
	4	17:35	36 16.14	73 58.86	500
ADCP	A	11:45:00 13:25:00	36 11.52 73 57.54	36 18.72 74 08.52	20
	B	16:30:00 17:30:00	36 22.32 74 07.32	36 16.26 73 58.86	16
	C	18:45:00 19:30:00	36 19.56 74 01.20	36 24.12 74 07.02	12
	D	21:15:00 23:00:00	36 24.72 74 02.82	36 15.58 74 50.58	25
RAR	19	16:06:32 16:15:25	36 34.58 74 13.02	36 02.58 74 13.02	54
	20	16:22:25 16:32:35	35 59.28 74 03.78	36 29.58 74 03.78	60
	22	16:45:08 16:55:07	36 24.08 74 53.22	36 09.60 74 23.70	60
	23	17:04:46 17:14:45	36 18.60 74 26.88	36 18.60 73 49.02	60
	24	17:24:04 17:32:59	36 26.28 73 51.12	36 26.28 74 30.72	54
	25	17:39:08 17:49:08	36 32.58 74 19.98	36 10.32 73 56.10	60

Table 4.1 Basic Statistics For the Marine Atmospheric Boundary Layer

Cold Side					
	N	Mean	Std Dev	Min	Max
Air Temperature	205	21.081	0.722	20.200	23.100
Wind speed	205	3.856	0.865	1.029	7.150
Wind direction	205	218.405	11.139	174.000	266.000
Wind stress	202	0.099	0.053	0.011	0.441
Sensible heat flux	205	-13.029	13.432	-46.216	24.669
Latent heat flux	205	-381.541	161.364	-962.455	58.236
Bulk Richardson Number	205	-0.589	1.148	-9.691	3.303
Surface roughness	205	0.033	0.011	0.009	0.098
Sea Surface Temperature	205	21.937	0.693	21.190	25.030
Salinity	205	33.201	0.330	32.550	34.540
Warm Side					
	N	Mean	Std Dev	Min	Max
Air Temperature	173	21.702	0.544	20.400	22.900
Wind speed	173	4.103	0.965	1.800	6.996
Wind Direction	173	208.571	12.684	187.000	248.000
Wind Stress	173	0.198	0.214	0.075	2.771
Sensible heat flux	173	-69.050	23.028	-156.896	-24.878
Latent heat flux	173	-461.072	140.538	-998.118	-186.271
Bulk Richardson Number	173	-2.898	1.658	-12.593	-0.517
Surface Roughness	173	0.053	0.076	0.032	1.033
Sea Surface Temperature	173	28.251	0.846	23.530	28.970
Salinity	173	36.102	0.394	33.460	36.260

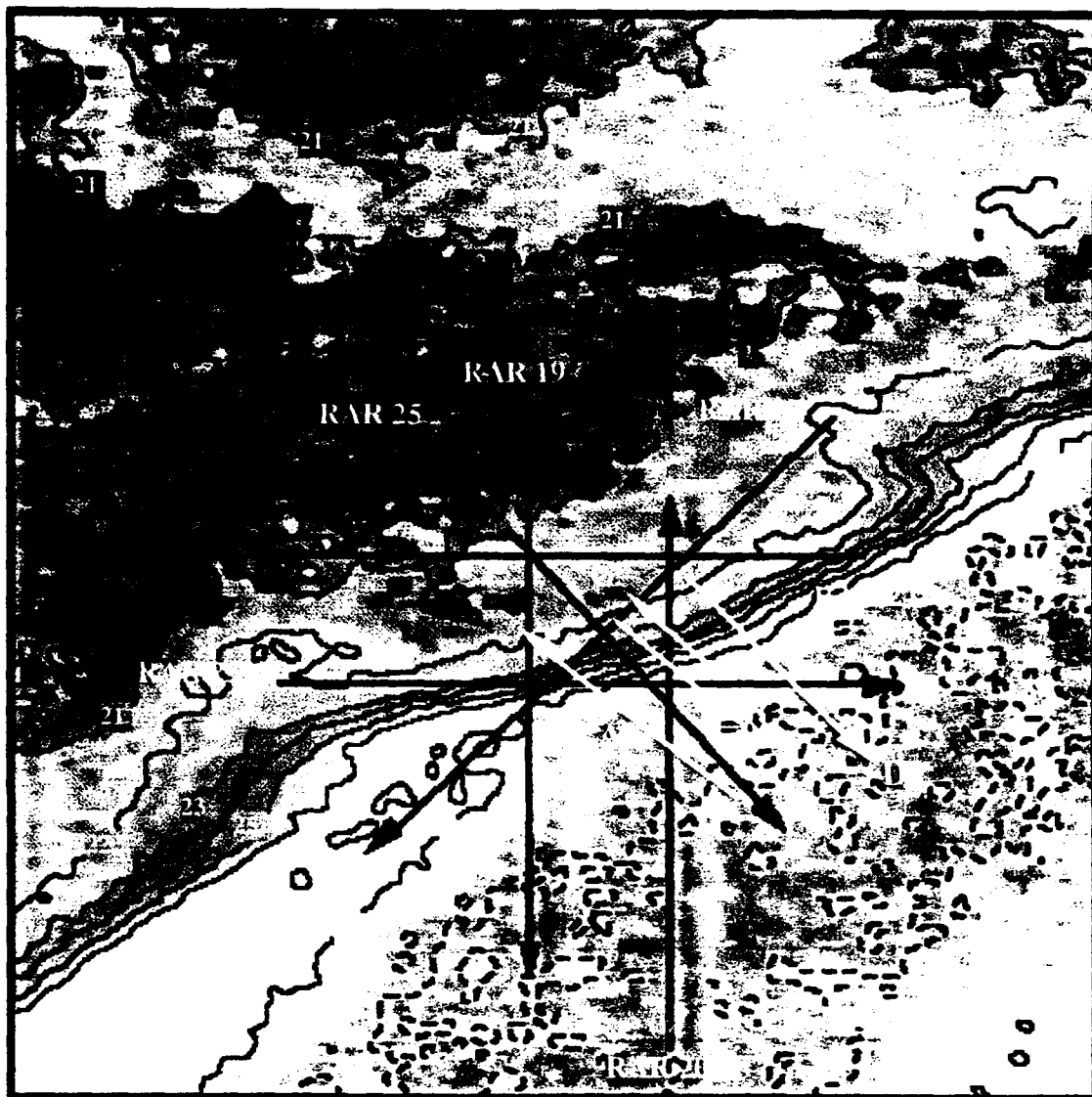


Figure 3.2

RAR flight tracts are denoted by the Black lines. RAR data was collected from the NRL RP3, between 16:00 and 18:00 GMT, on 3 October, 1990. RAR imagery was acquired from an average altitude of 175 m at low resolution and at intermediate to low grazing angles. ADCP Tracks, denoted by the white lines, were collected between 11:30 and 23:00. The only sea truth data concurrent with the RAR over flights was collected during track B.

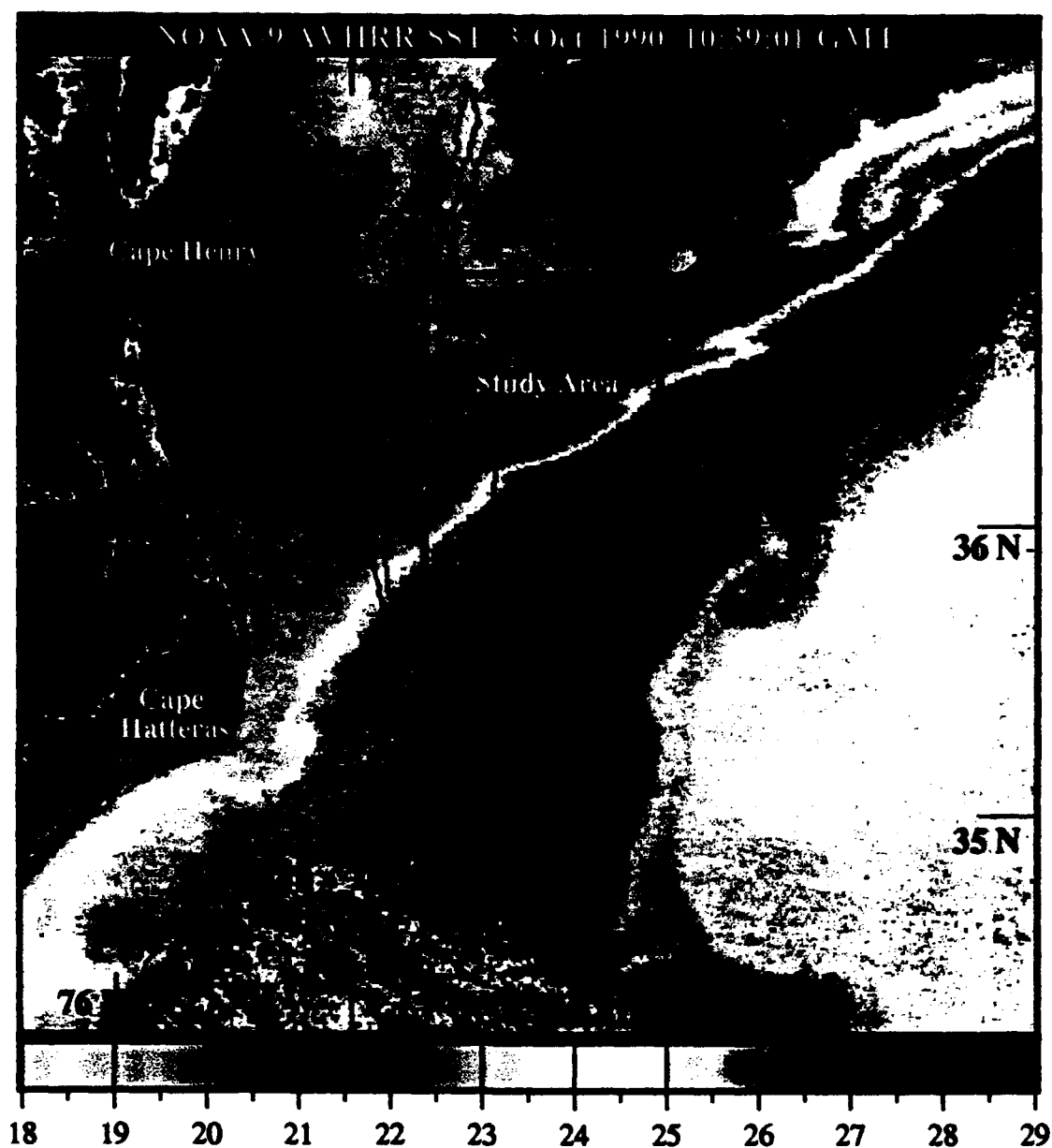


Figure 3.1

Region of airborne and shipboard operations on 3 October, 1990. The Gulf Stream is indicated by the orange and red regions. Cooler waters of the mid and outer MAB shelf are denoted by the light blue regions. The darker green regions, between Cape Hatteras and Cape Henry, and shoreward of the Gulf Stream are mixtures of estuarine discharges from the Chesapeake and Delaware.

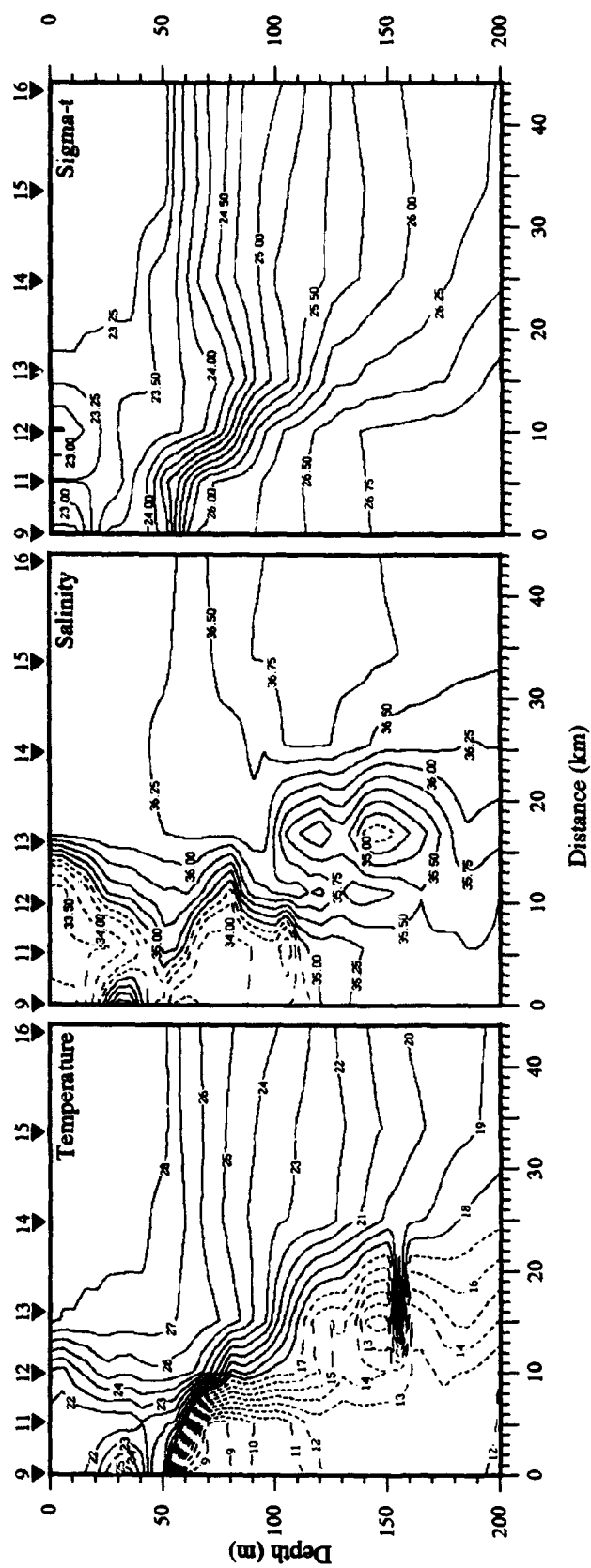


Figure 4.3 Temperature, salinity, and sigma-t cross-sections from CTD stations 9 to 16, collected on 3 October, 1990

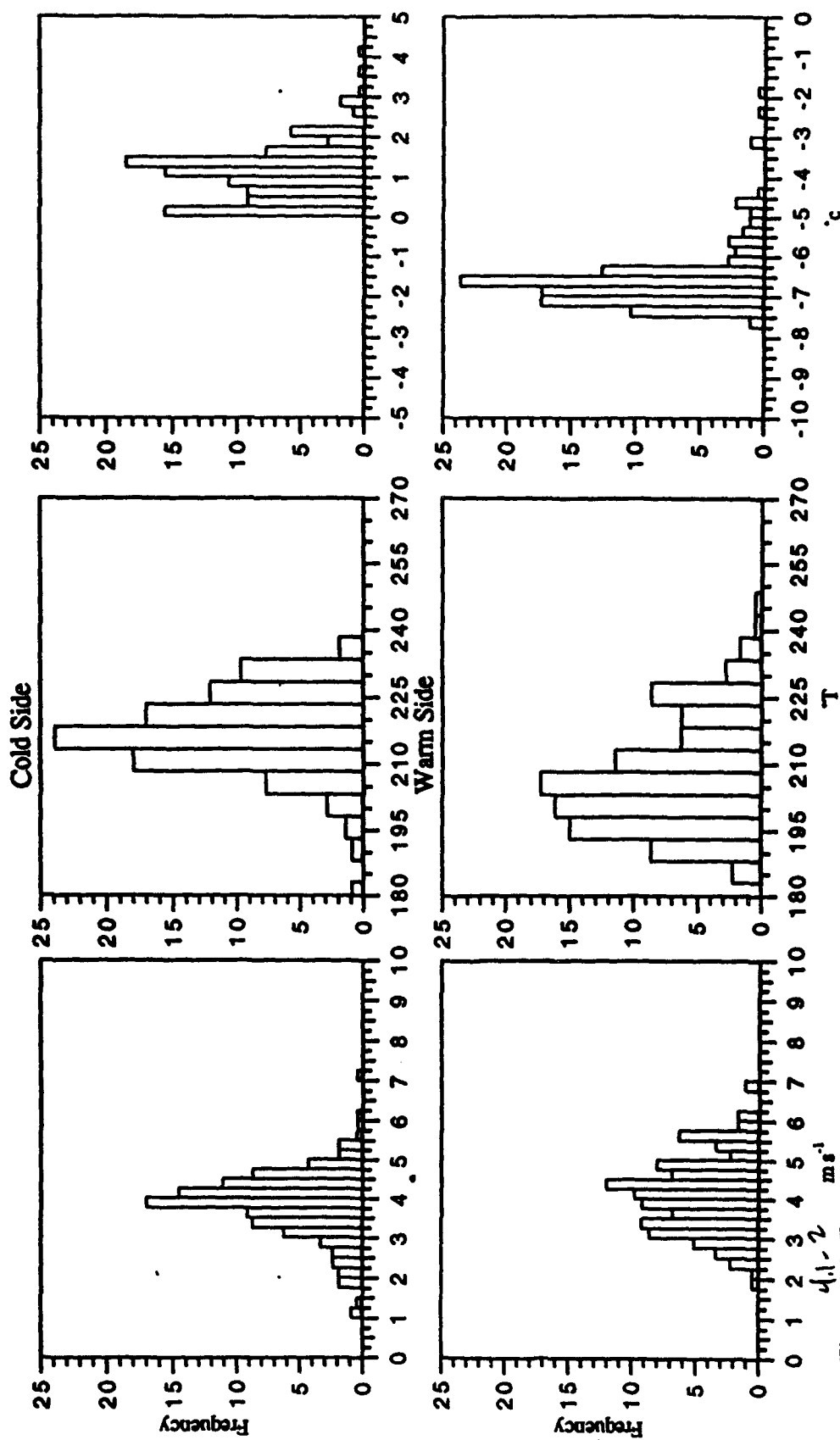
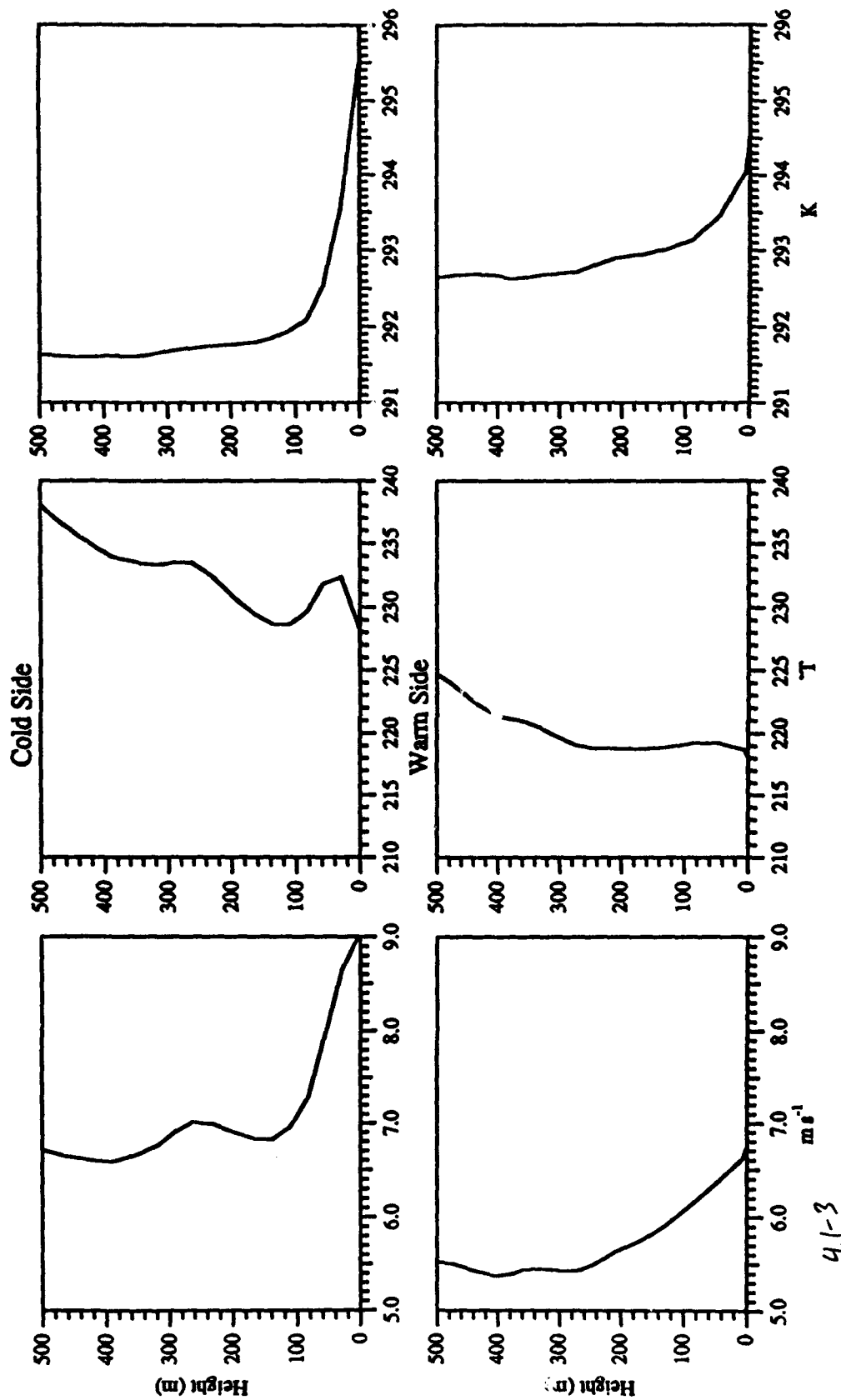


Figure 4.1 Frequency distributions of wind speed, wind direction, and air-sea temperature difference for cold and warm side Gulf Stream frontal observations between 11:00 and 23:00 gmt, on 3 October, 1990.



4.1-3

Figure 4.2 Vertical Soundings of wind speed, wind direction, and potential temperature for cold and warm side observation

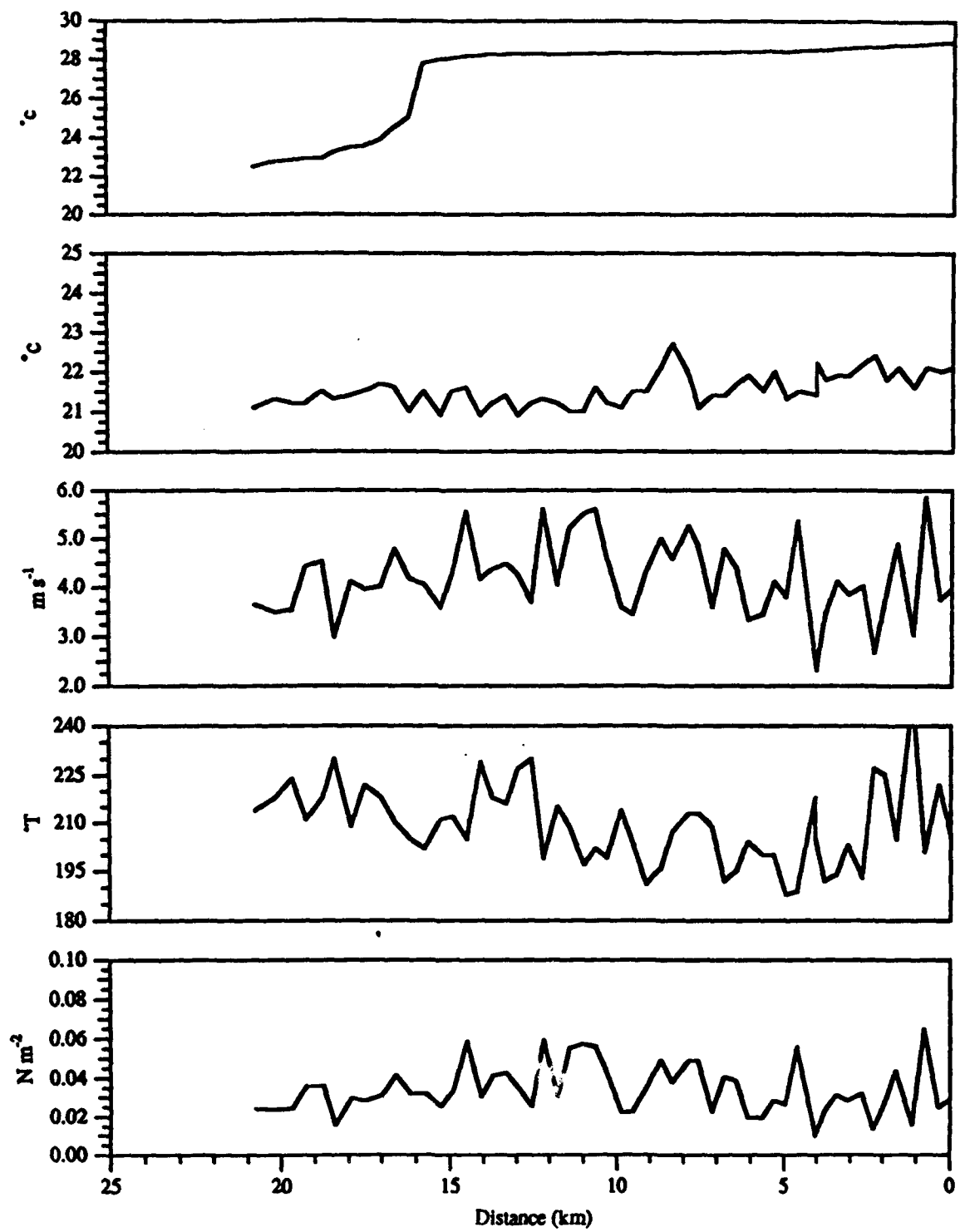


Figure 4.1-1a Ship Track A: MABL Measurements. SST, Air temperature, Wind speed, Direction, and stress

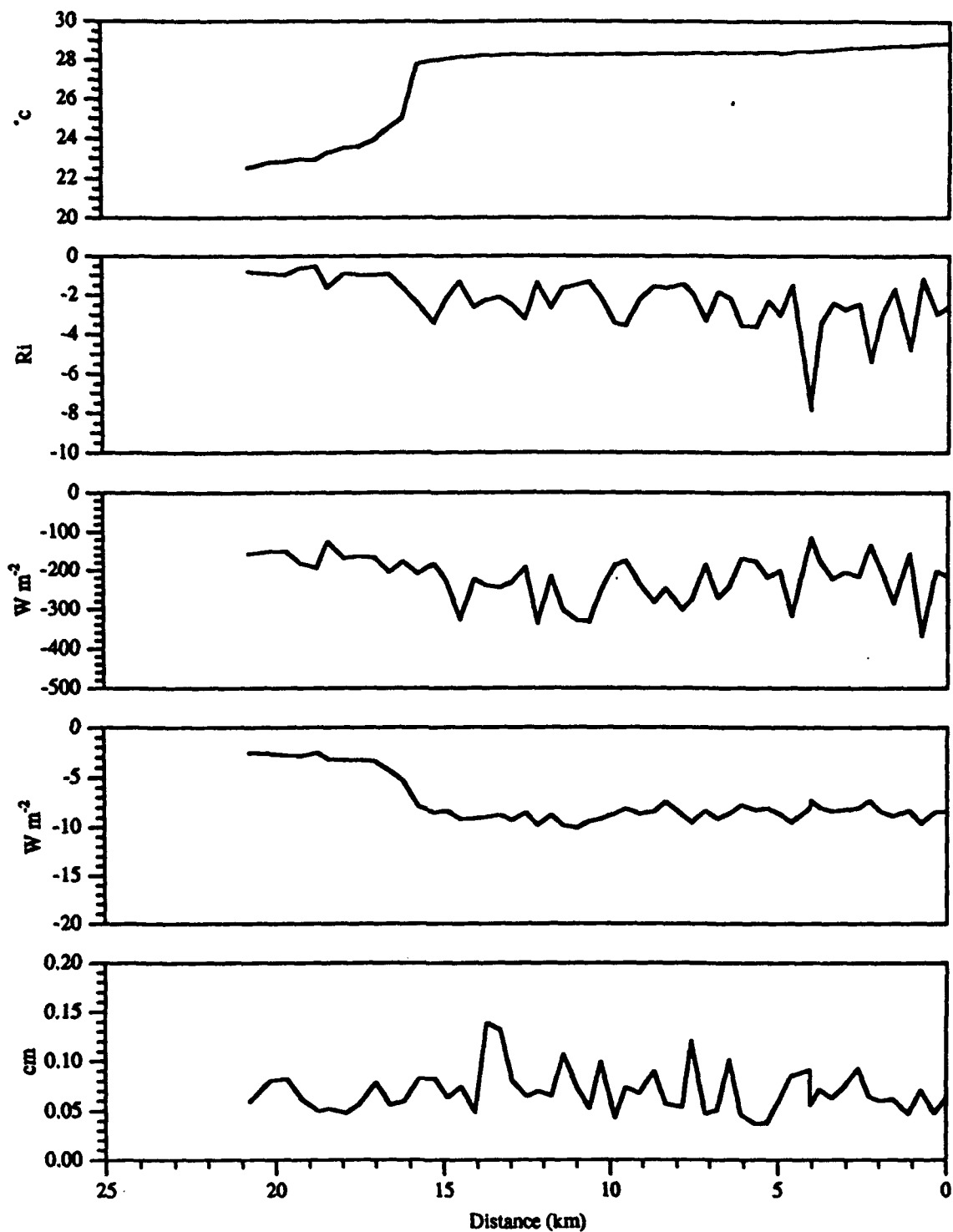


Figure 4.1-1b Ship Track A: MABL Measurements. SST, Bulk Richardson, Number Sensible Heat Flux, Latent Heat Flux, and Surface Roughness

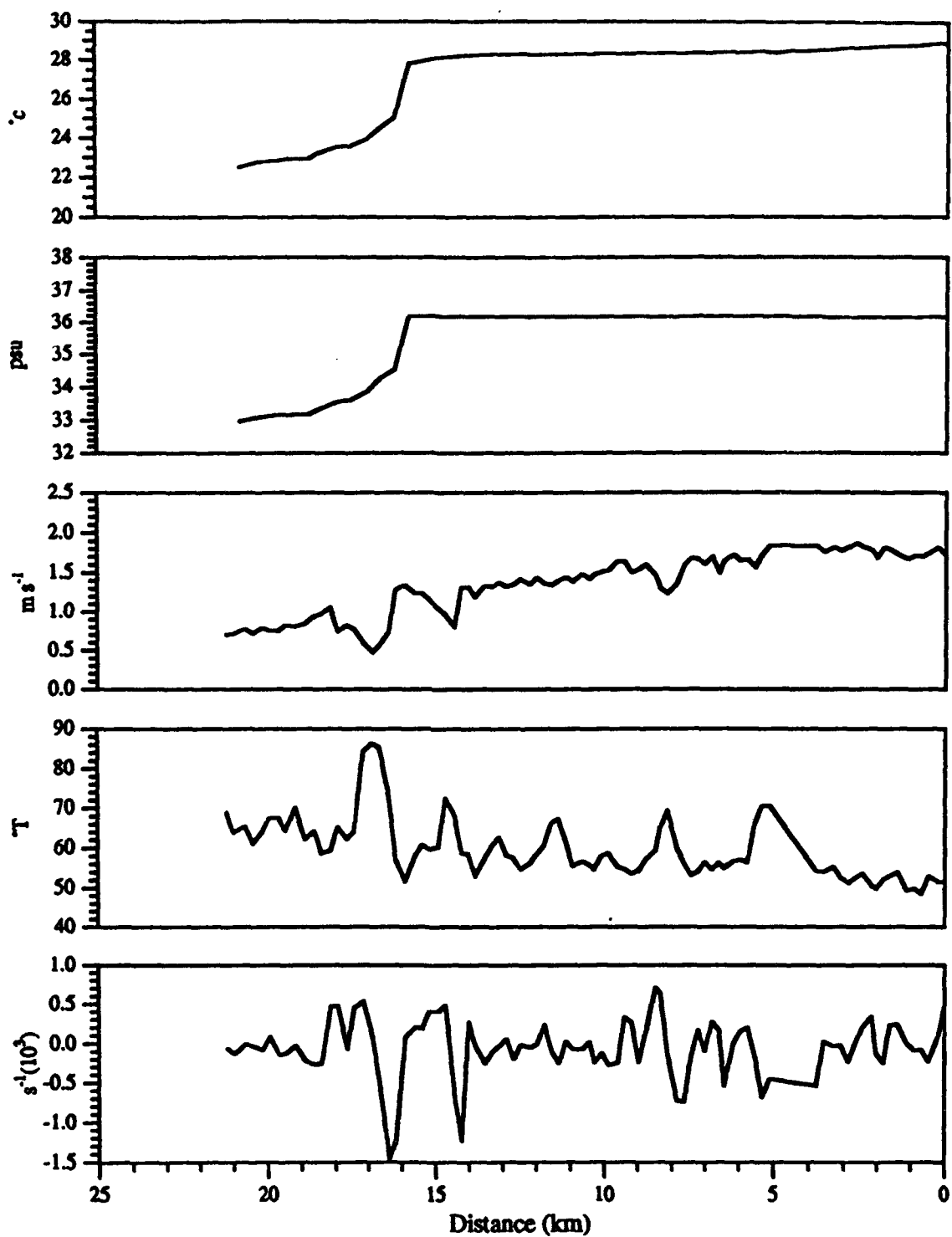


Figure 4.1-1a ADCP Track A: Oceanic Mixed layer Measurements.
SST, Salinity, Current speed, Direction, And Shear at 8 m

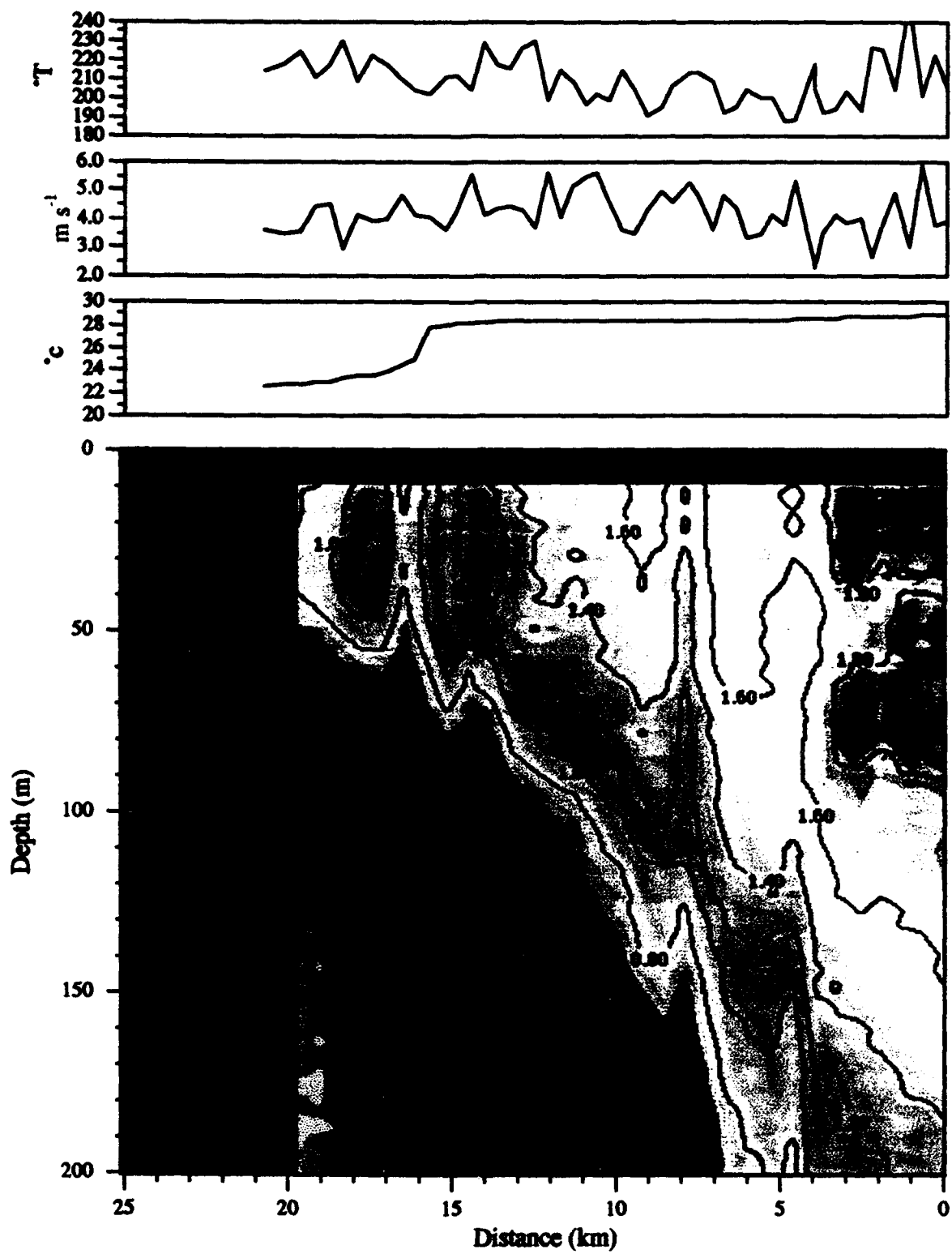


Figure 4.2 b. ADCP Profile for ship track A

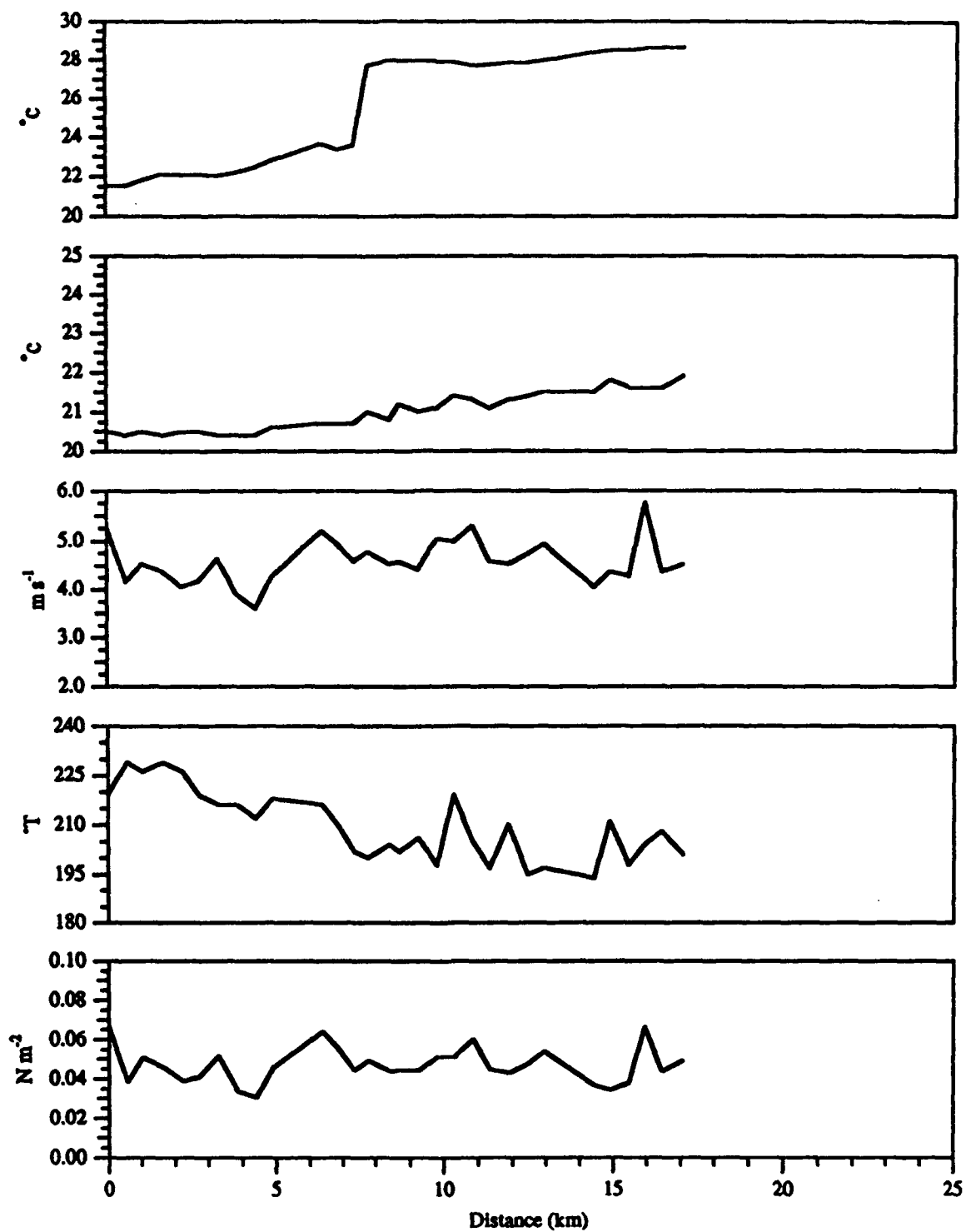


Figure 4.1-2a Ship Track B: MABL Measurements. SST, Air temperature
Wind speed, Direction, and stress

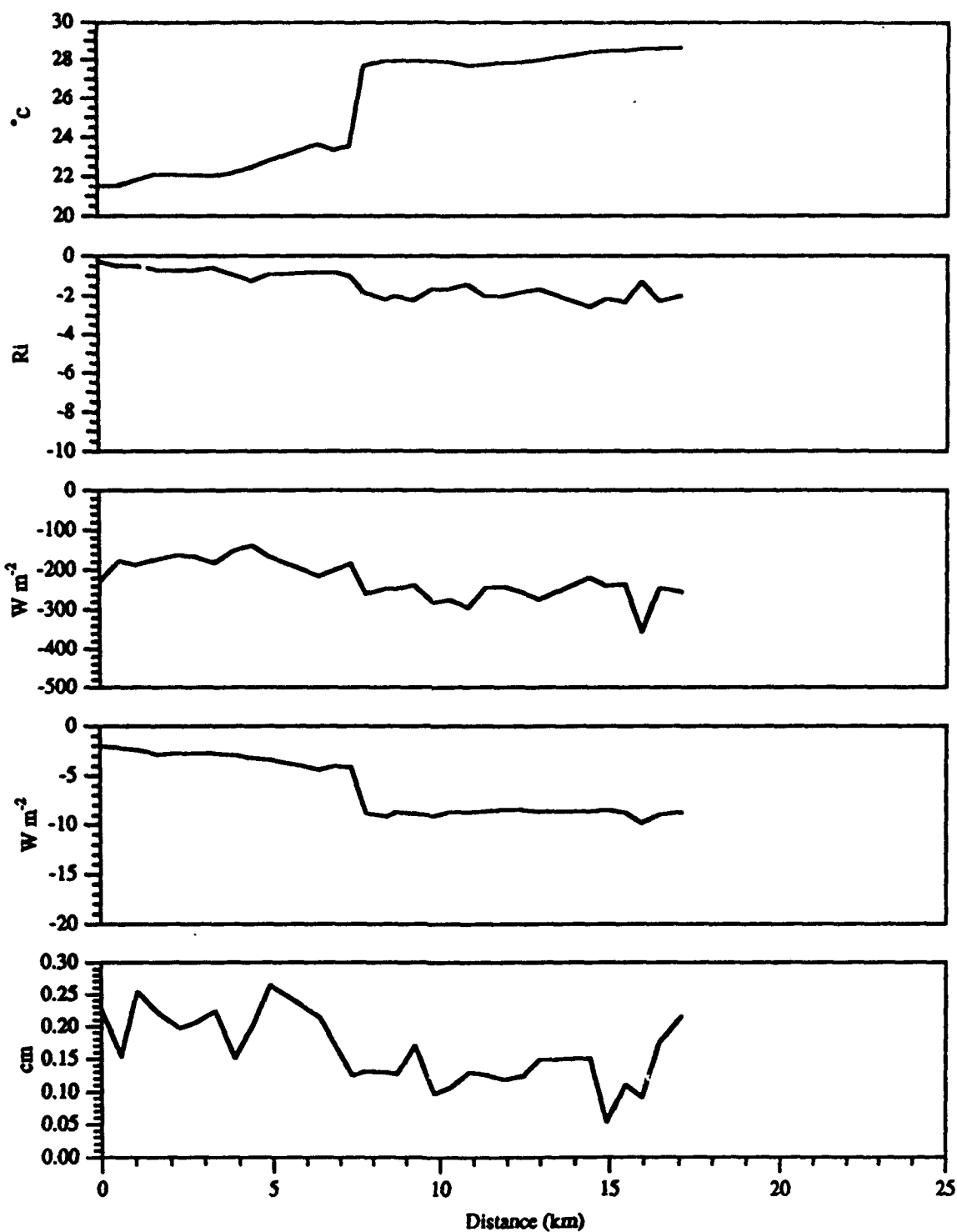


Figure 4.1-2b Ship Track B: MABL Measurements. SST, Bulk Richardson, Number Sensible Heat Flux, Latent Heat Flux, and Surface Roughness

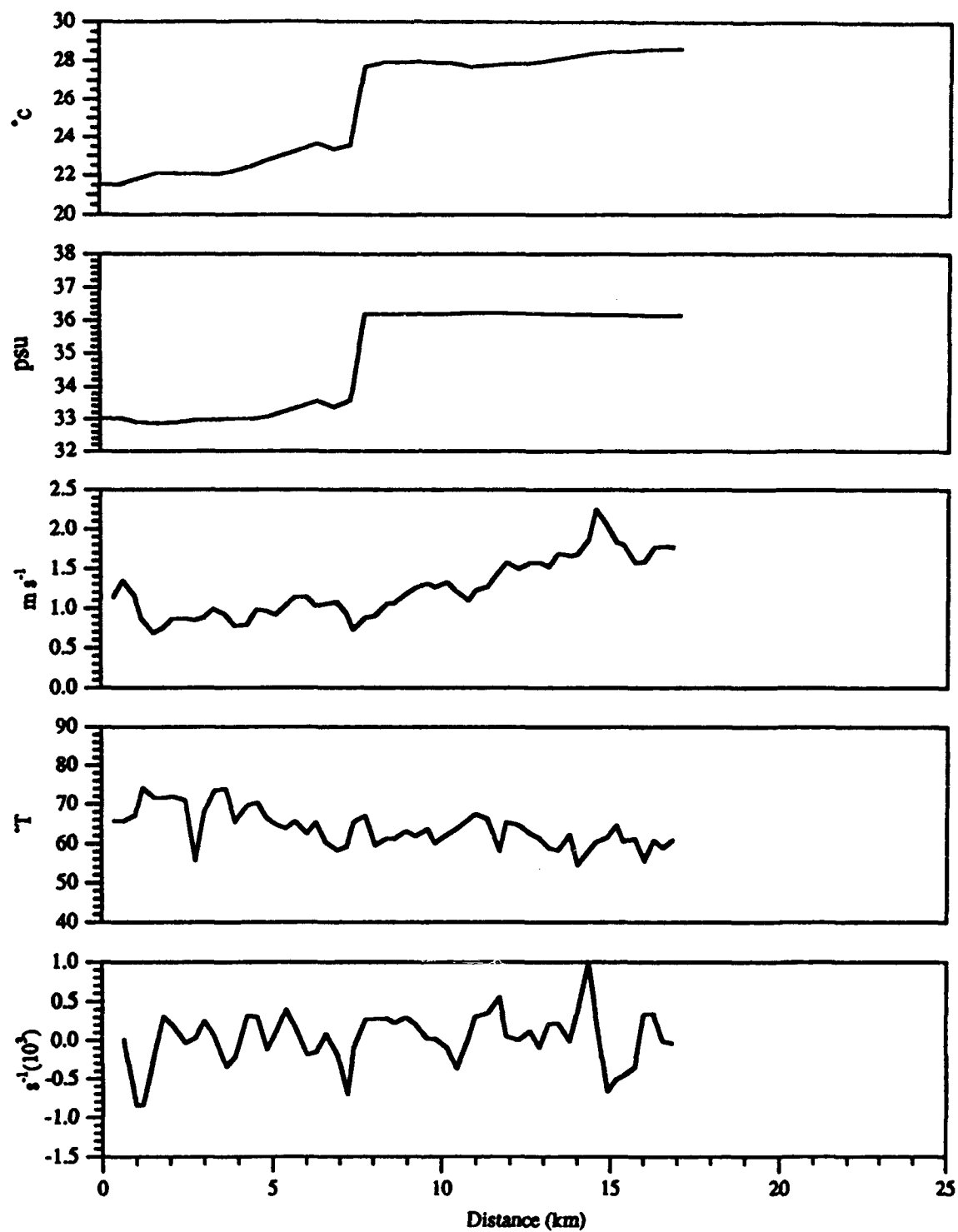


Figure 4.1-2c Ship Track B: Oceanic Mixed layer Measurements.
SST, Salinity, Current speed, Direction, And Shear at 8 m

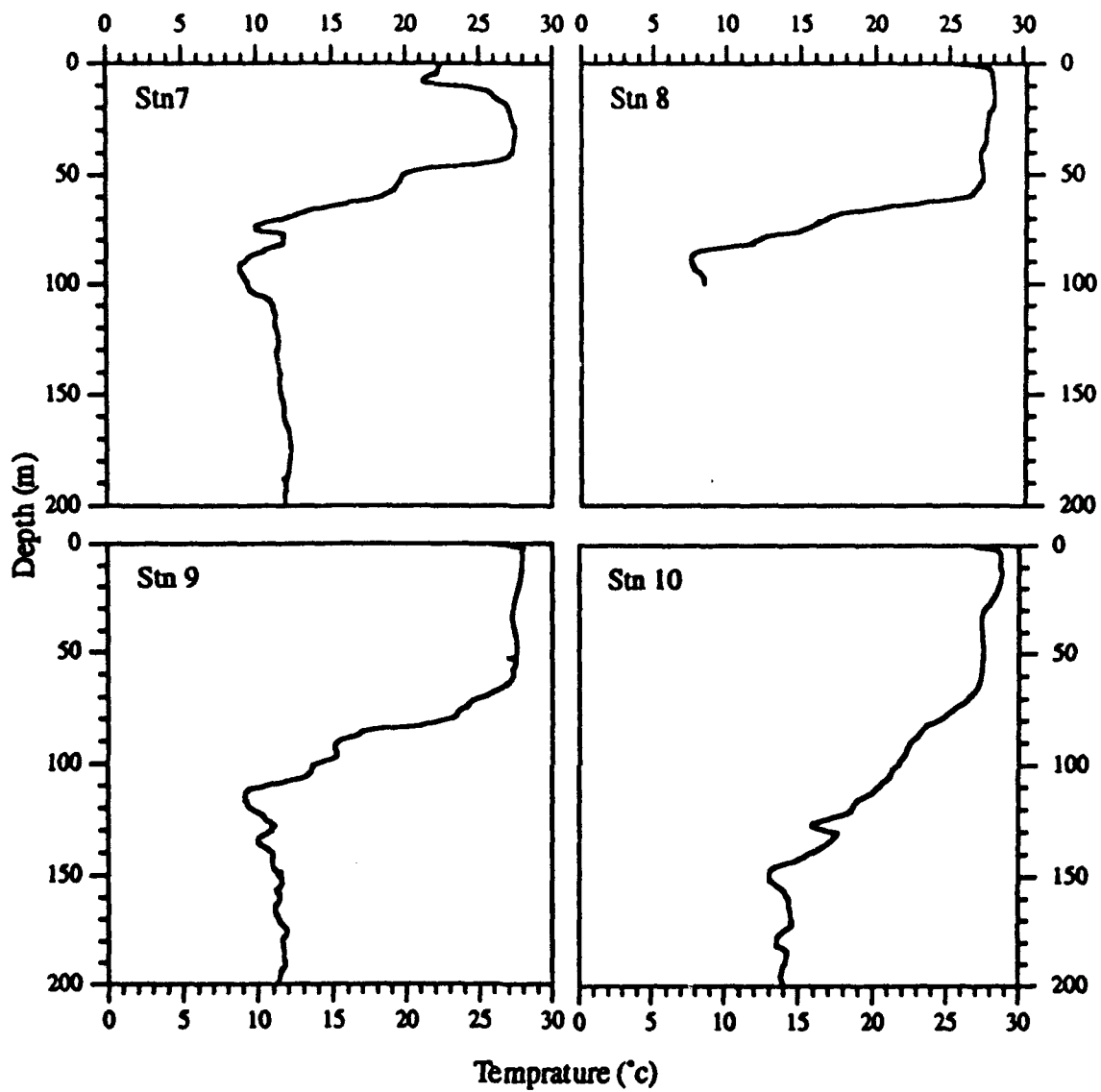


Figure 4.1-2d XBT profiles acquired during ship track B

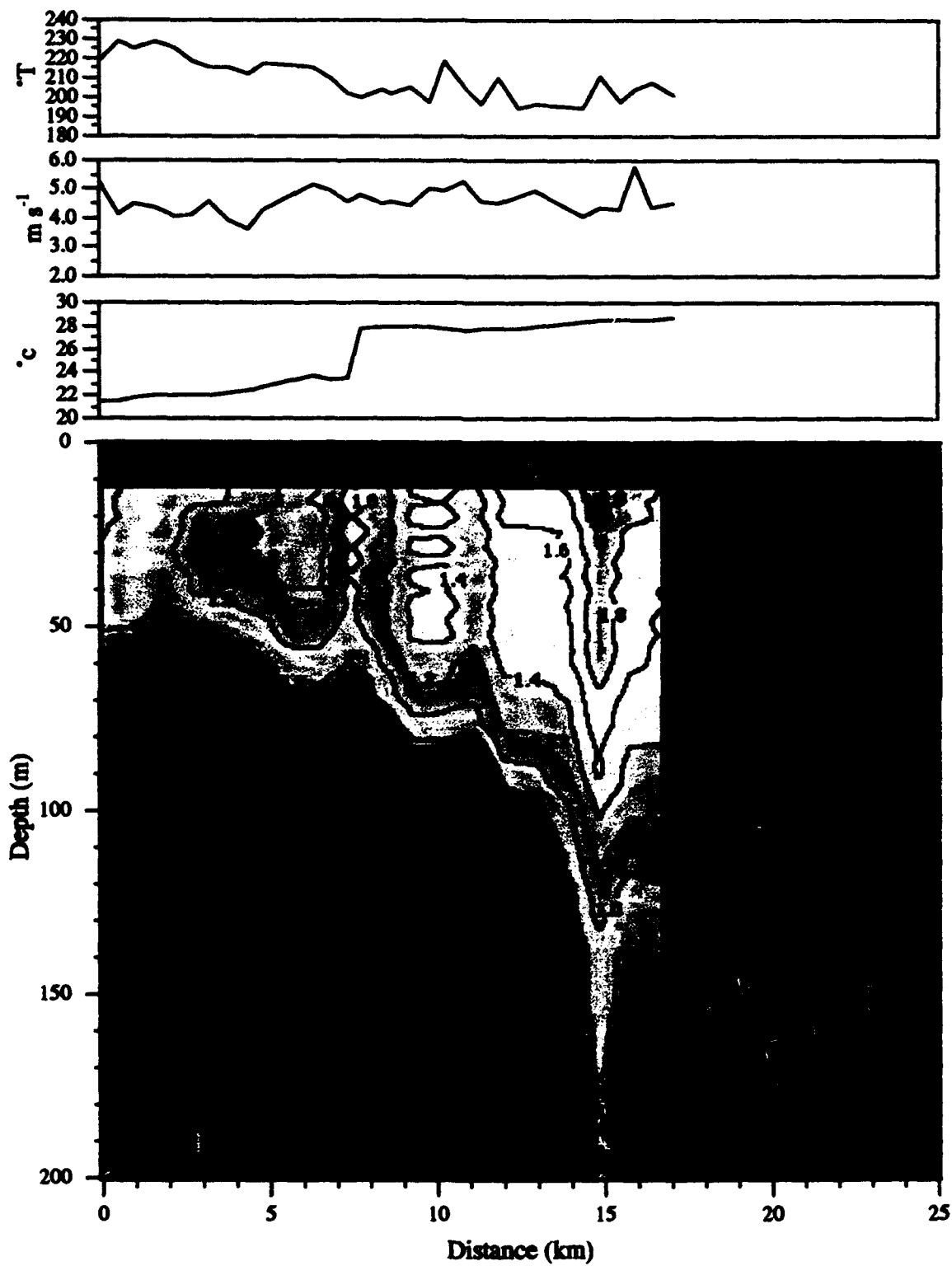


Figure 4.3 b ADCP profile for ship track B.

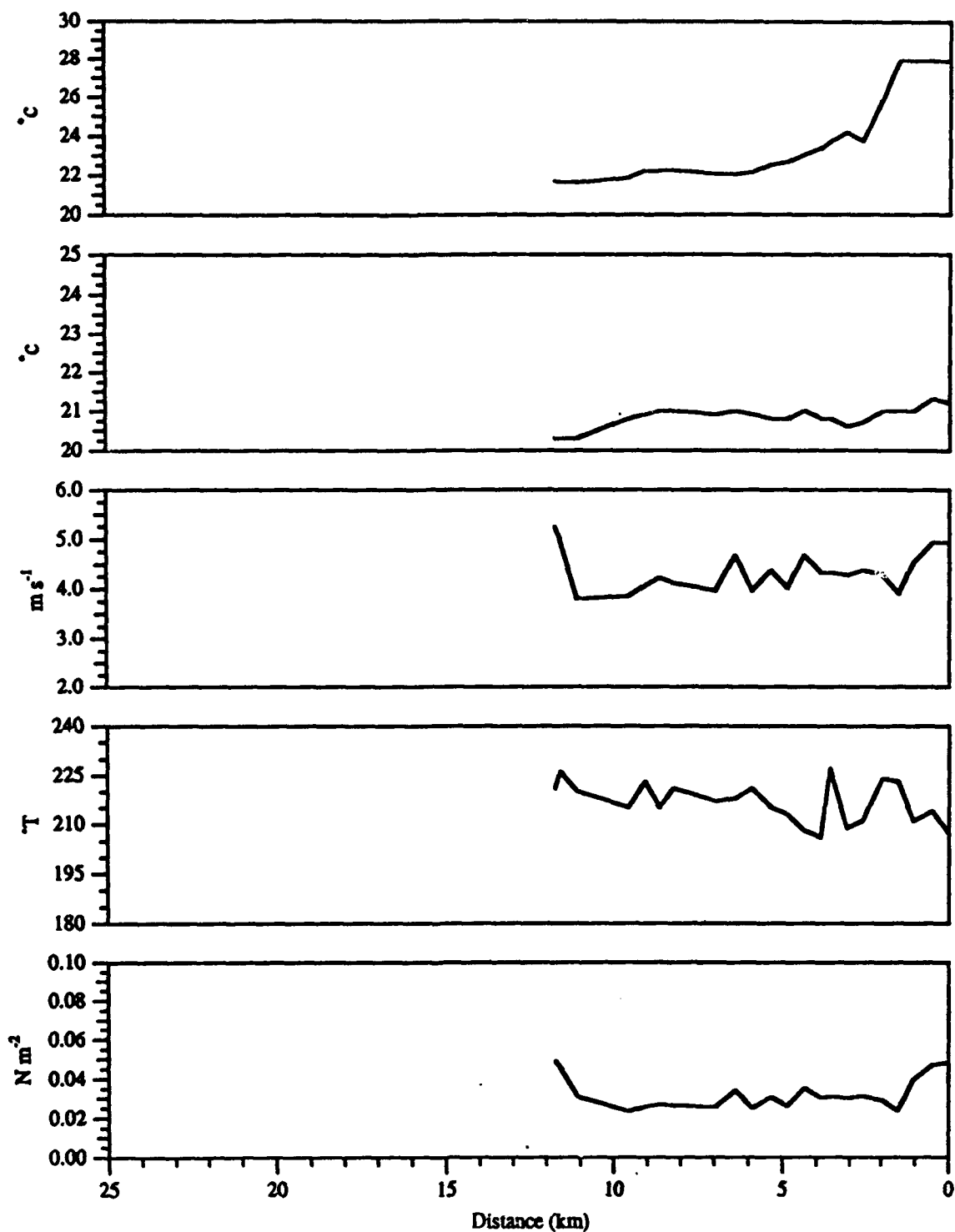


Figure 4.1-3a Ship Track C: MABL Measurements. SST, Air temperature
Wind speed, Direction, and stress

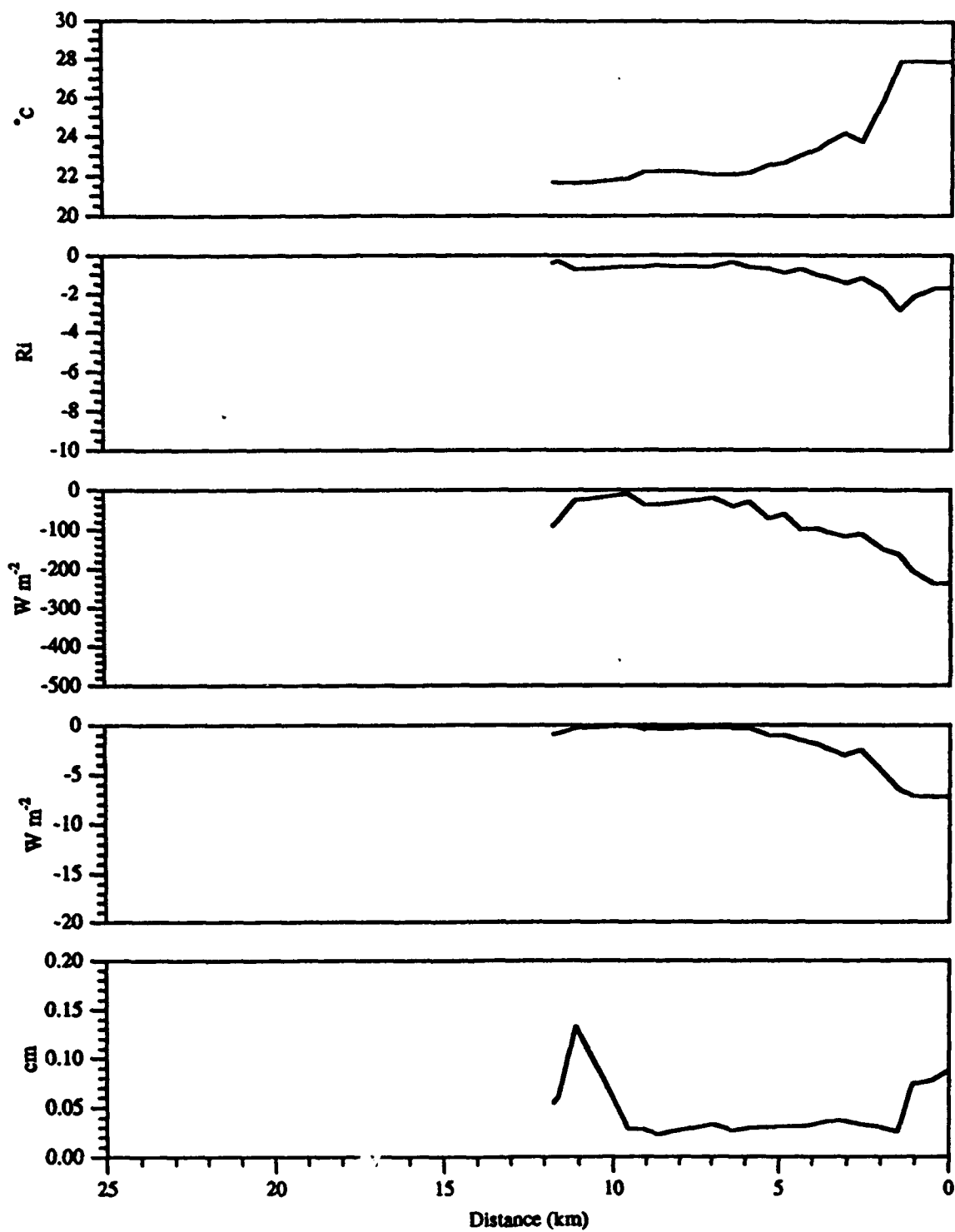


Figure 4.1-3b Ship Track C: MABL Measurements. SST, Bulk Richardson, Number
Sensible Heat Flux, Latent Heat Flux, and Surface Roughness

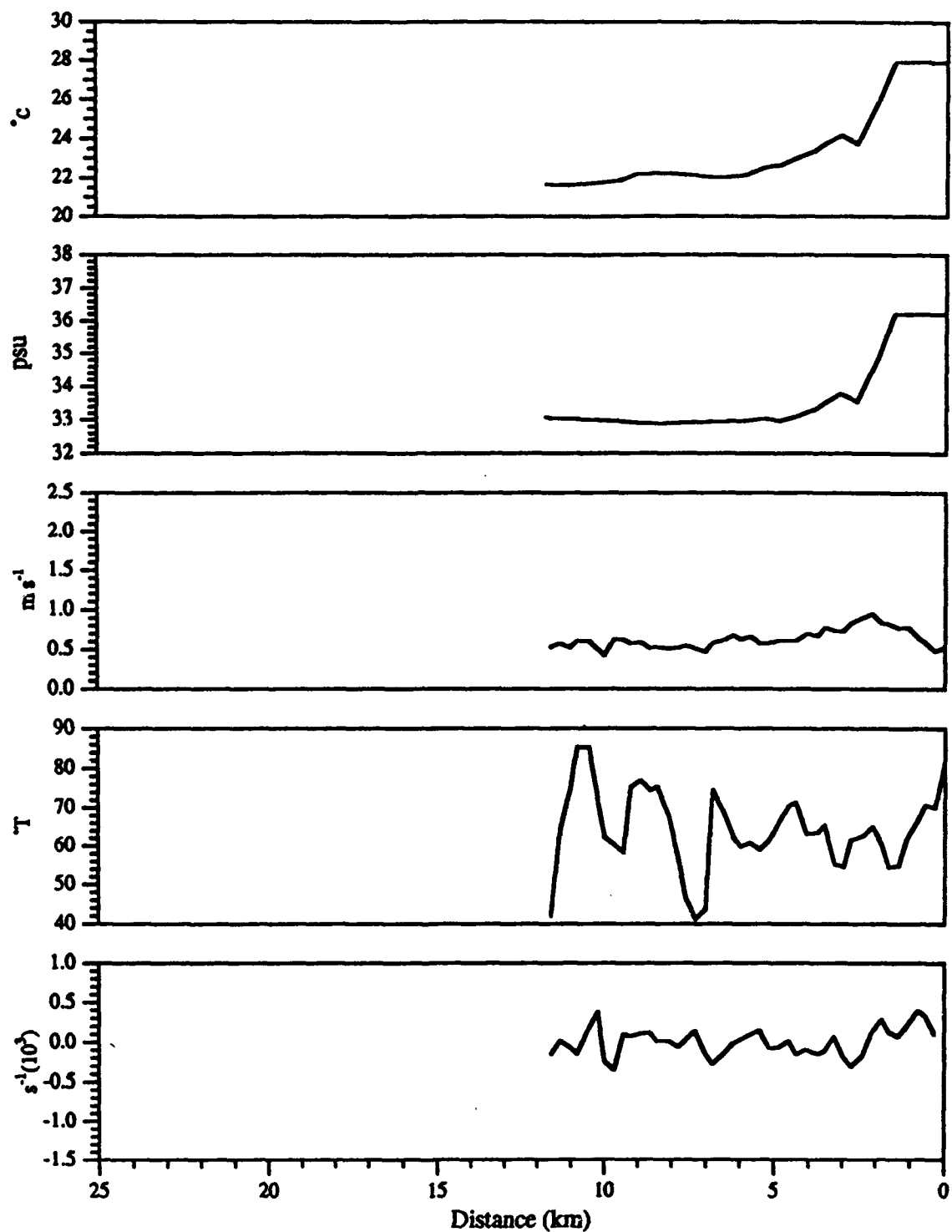


Figure 4.1-3a Ship Track C: Oceanic Mixed layer Measurements.
SST, Salinity, Current speed, Direction, And Shear at 8 m

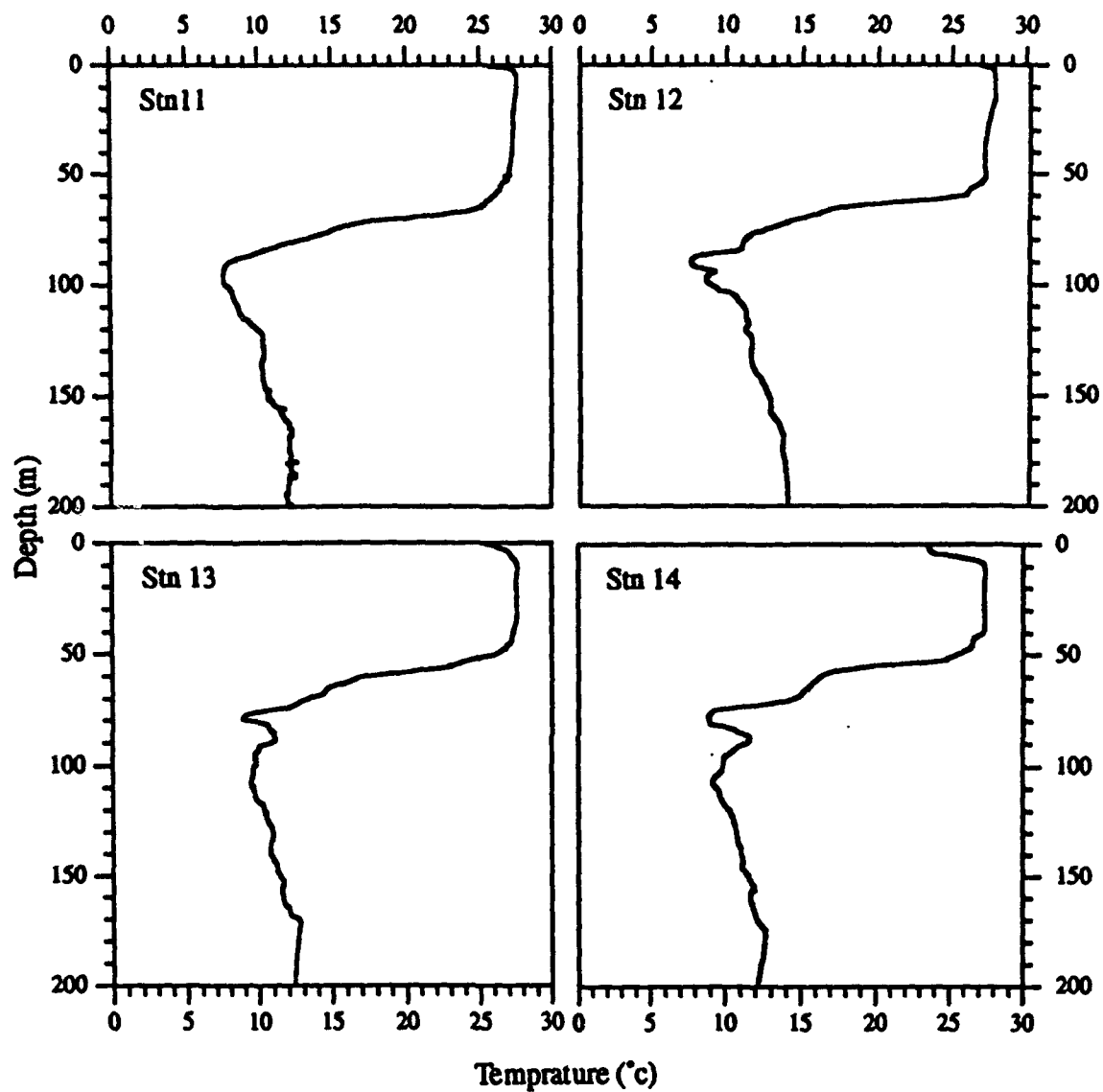


Figure 4.1-2d XBT profiles acquired during ship track c

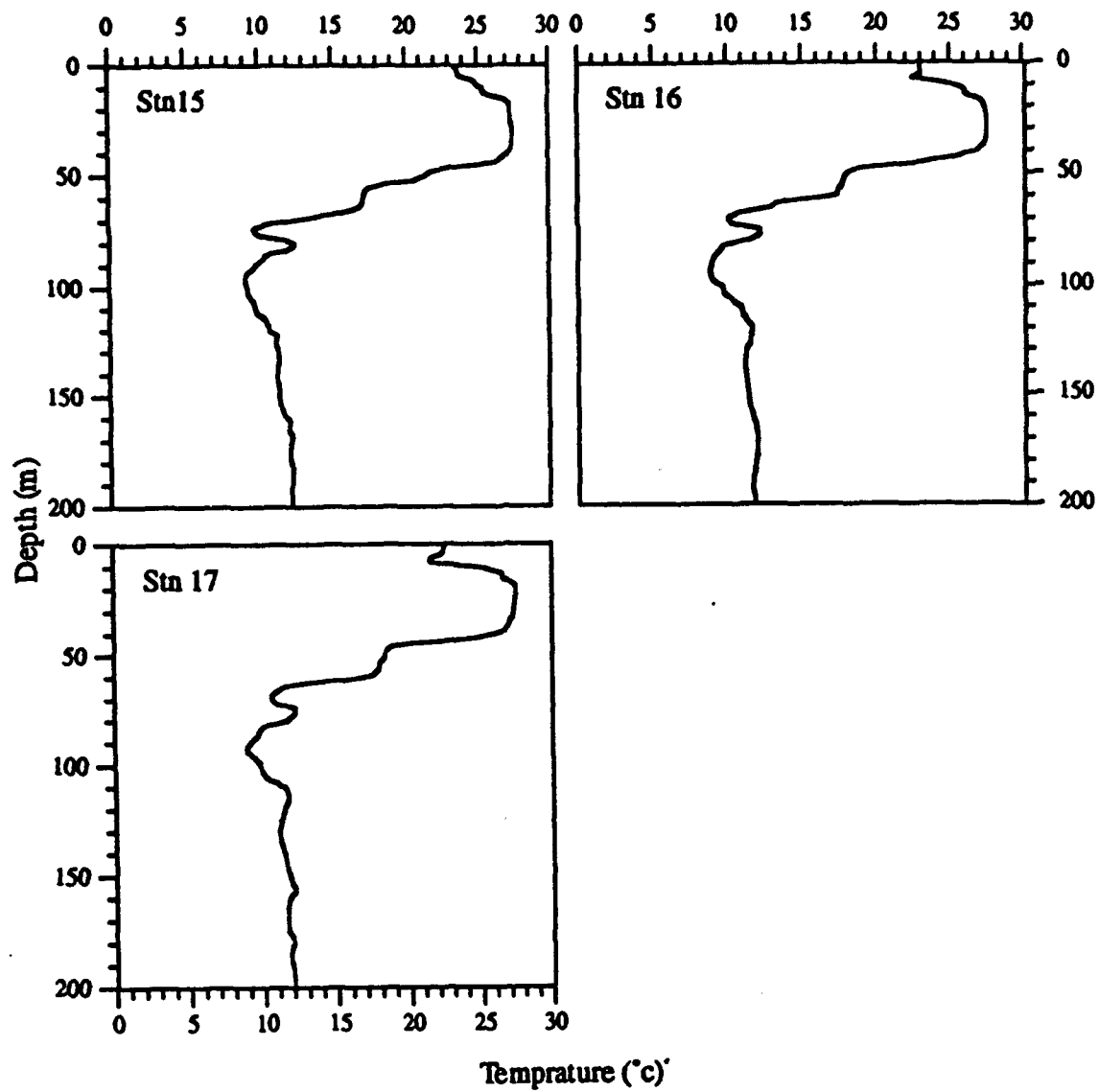


Figure 4.1-2d XBT profiles acquired during ship track C

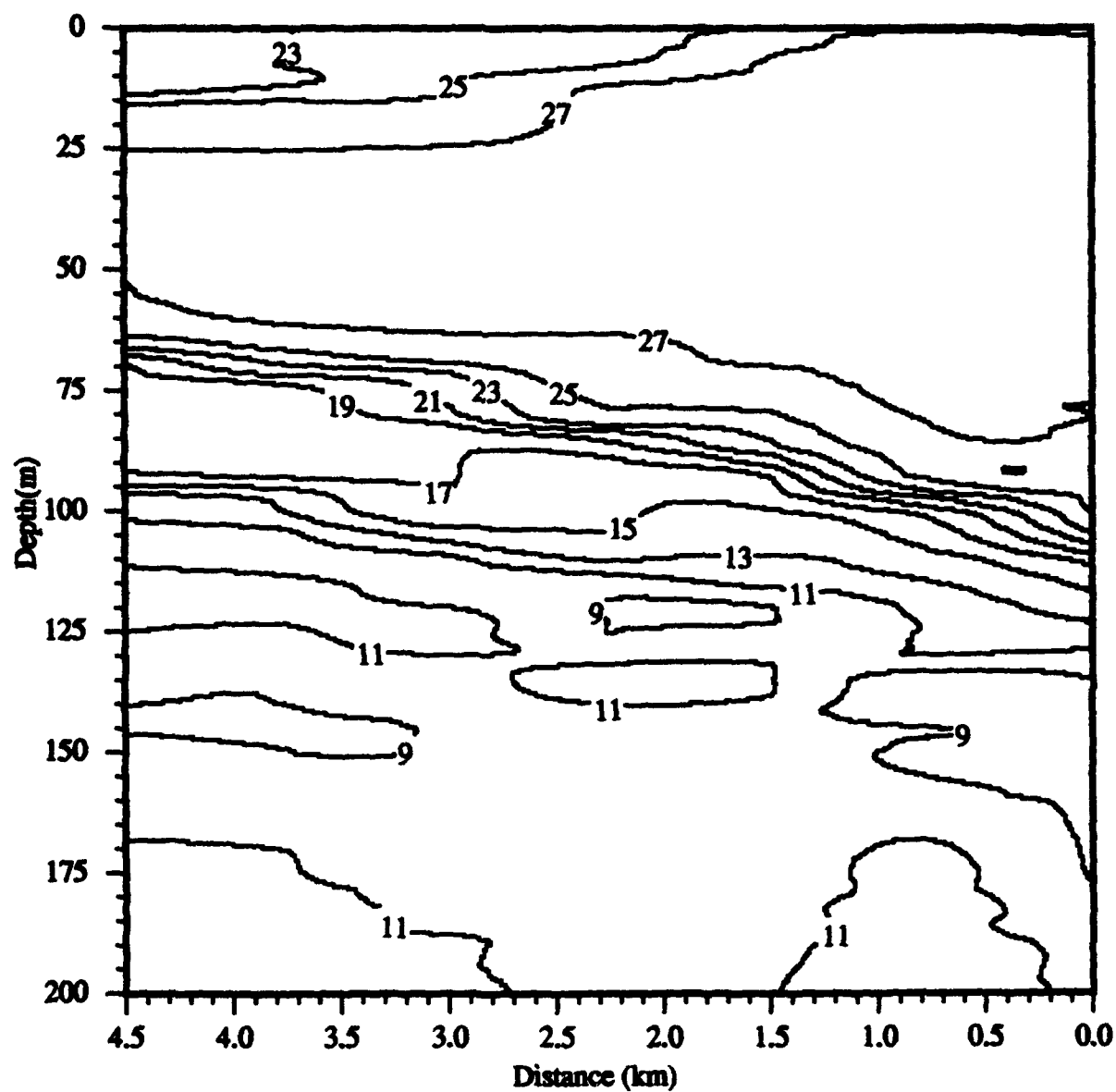


Figure 4.1-4d XBT temperature profile from ship Track C.

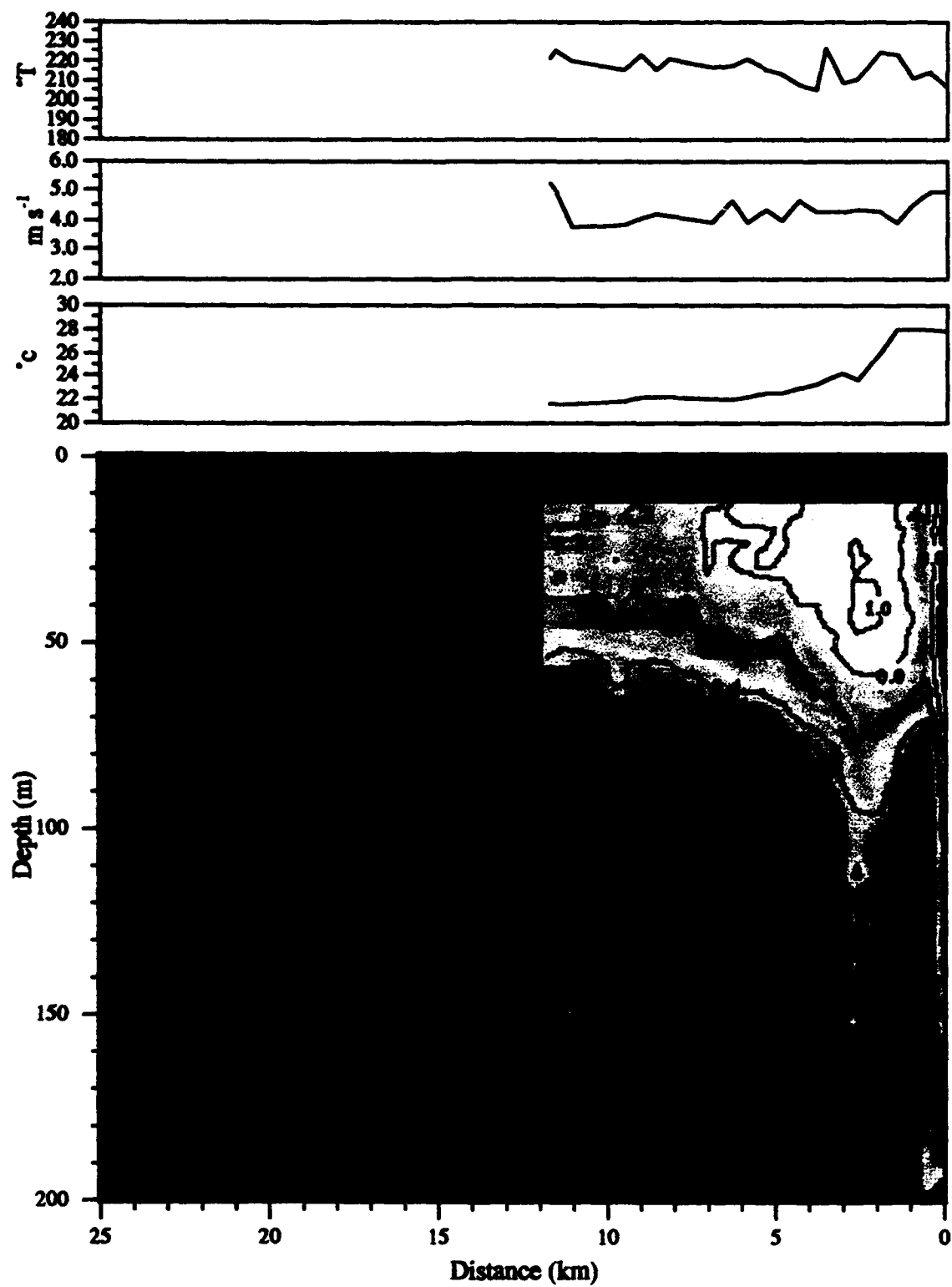


Figure 4.2 b. ADCP Profile for ship track c

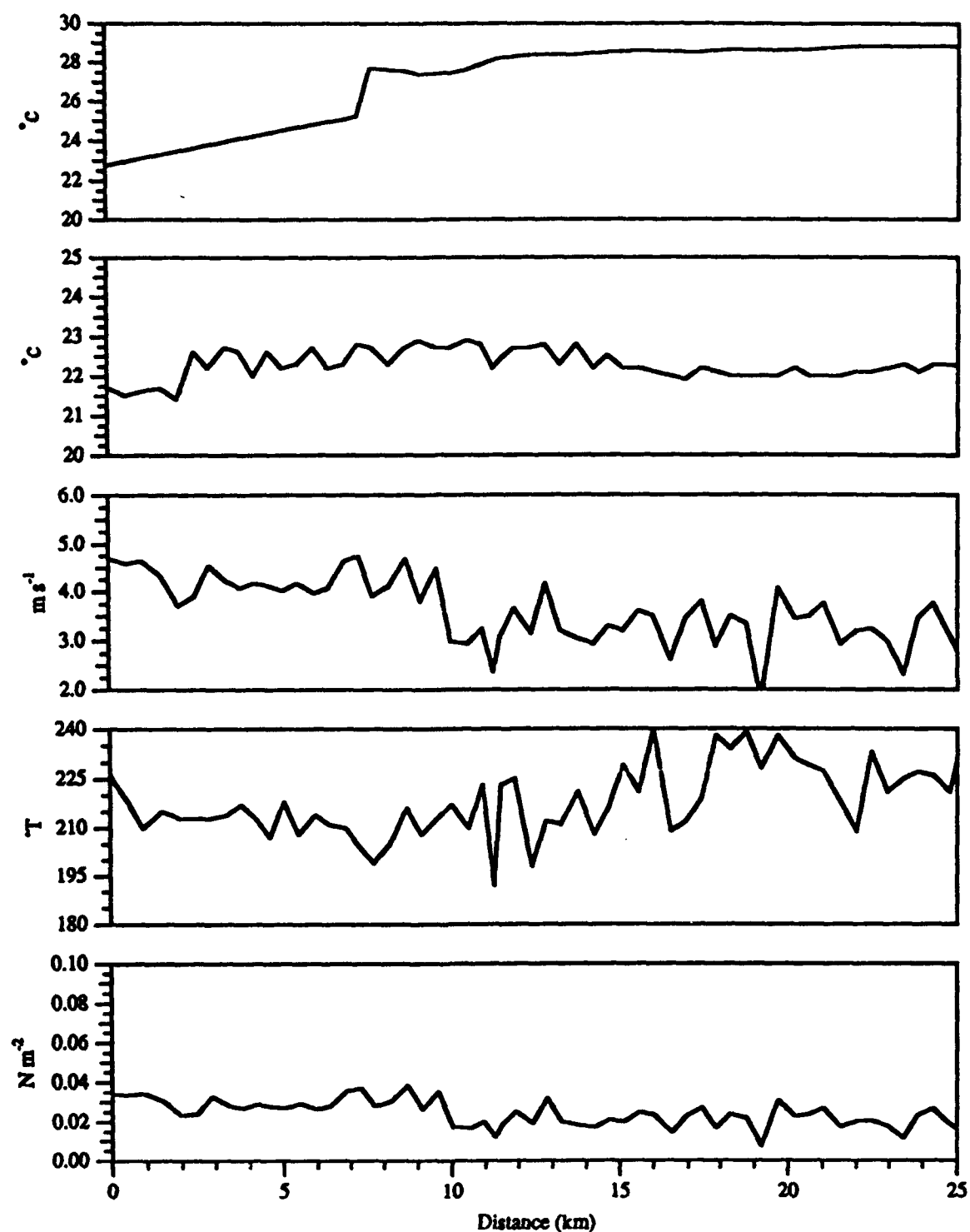


Figure 4.1-4a Ship Track D: MABL Measurements. SST, Air temperature
Wind speed, Direction, and stress

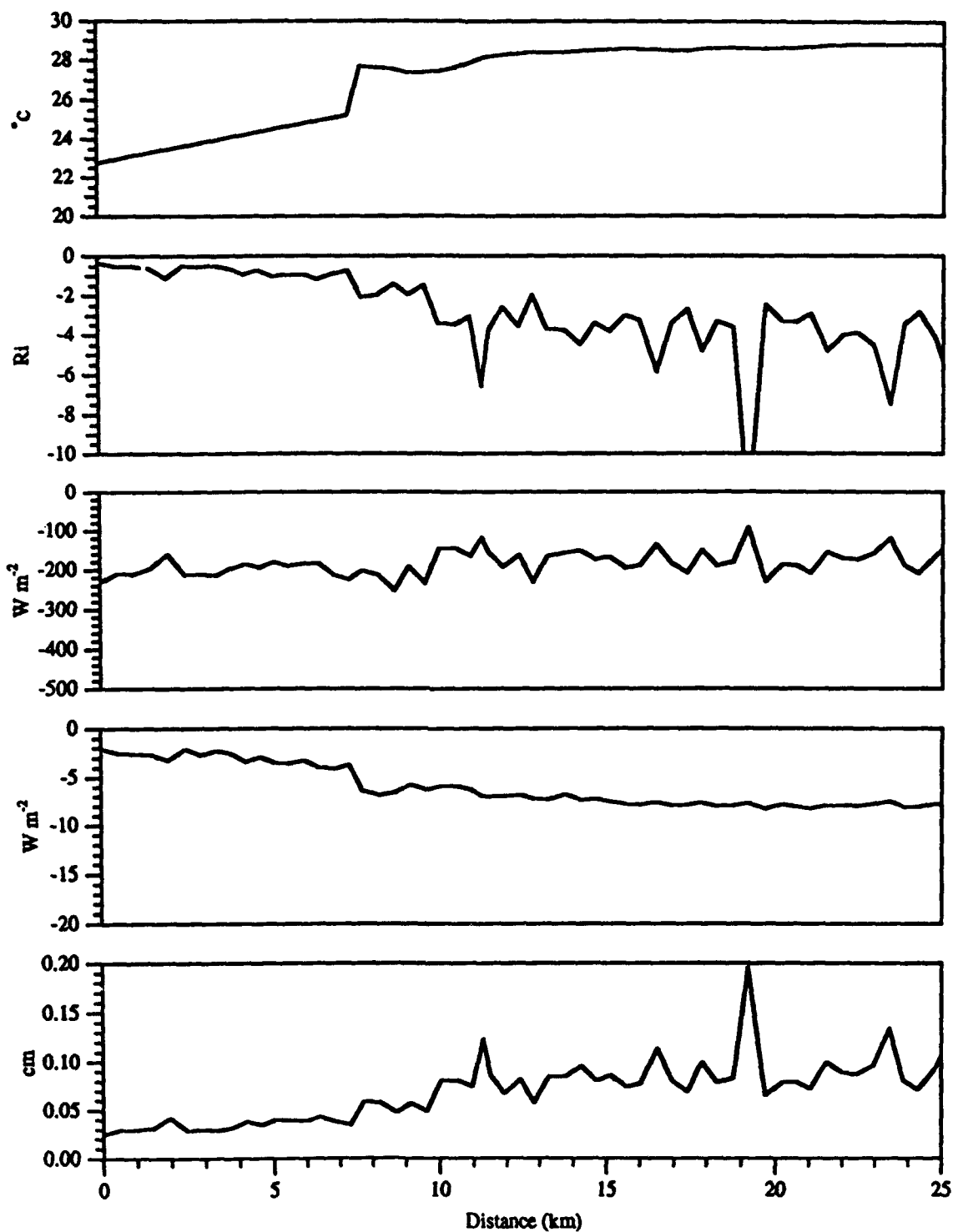


Figure 4.1-4b Ship Track D: MABL Measurements. SST, Bulk Richardson, Number Sensible Heat Flux, Latent Heat Flux, and Surface Roughness

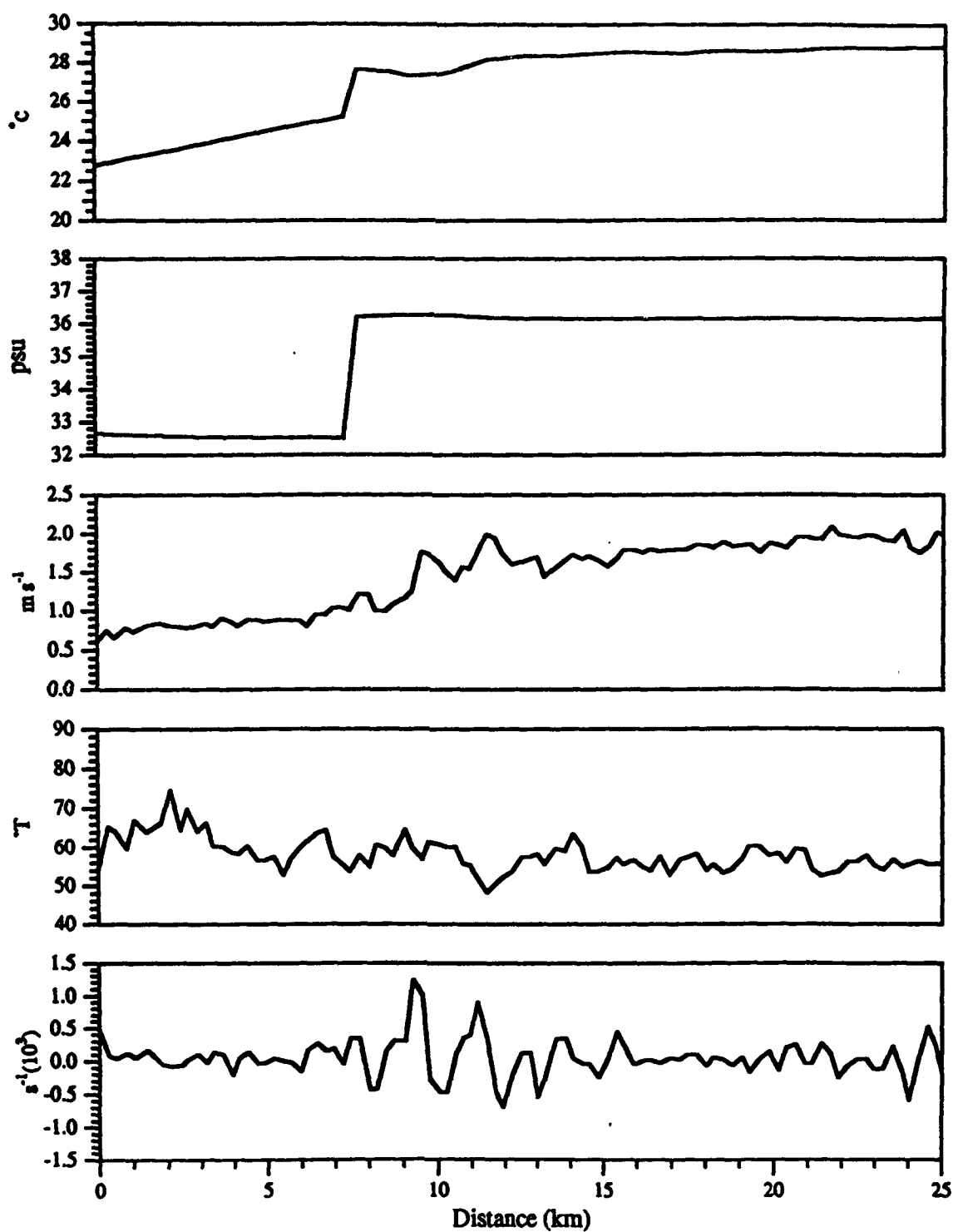
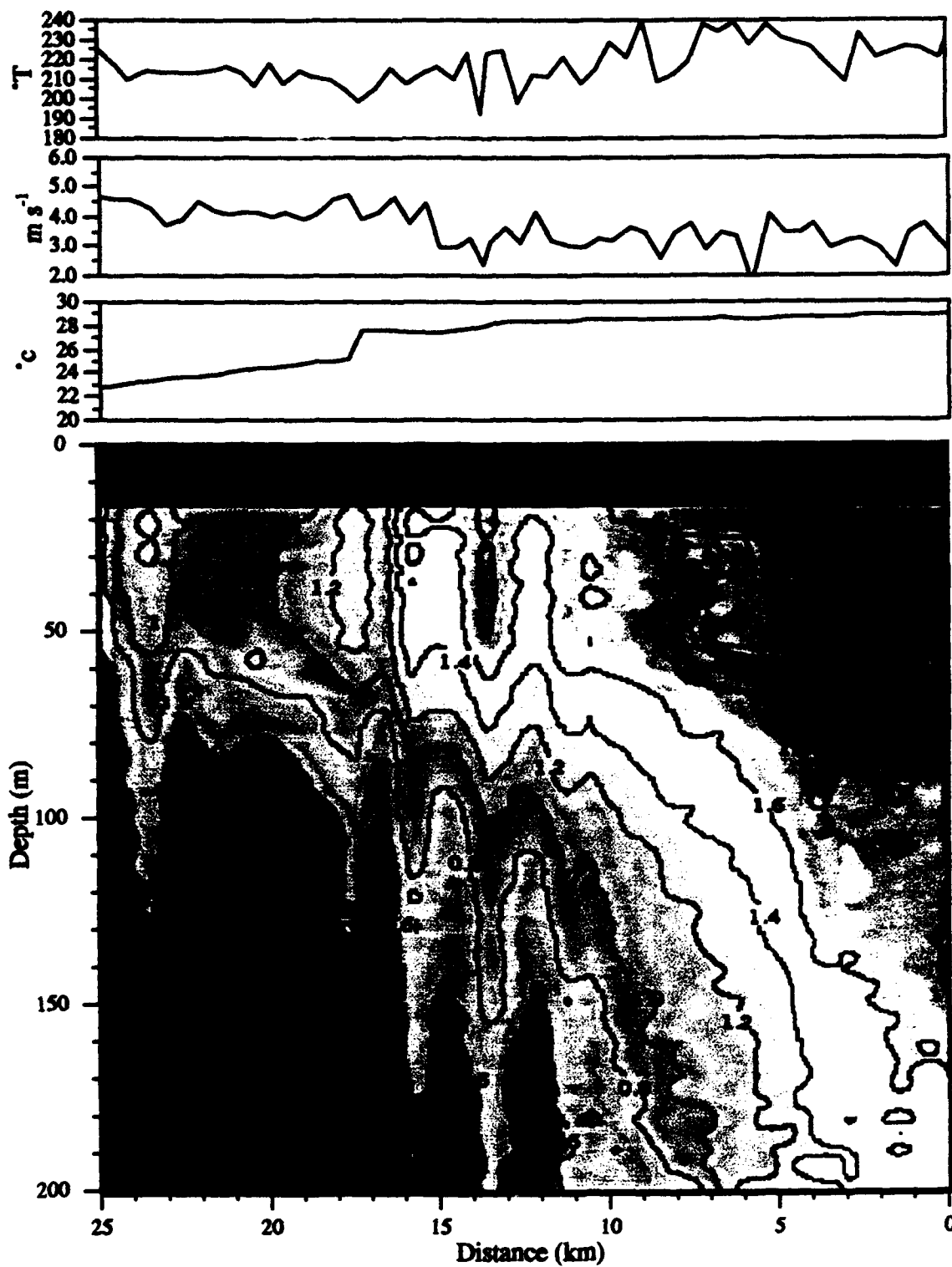
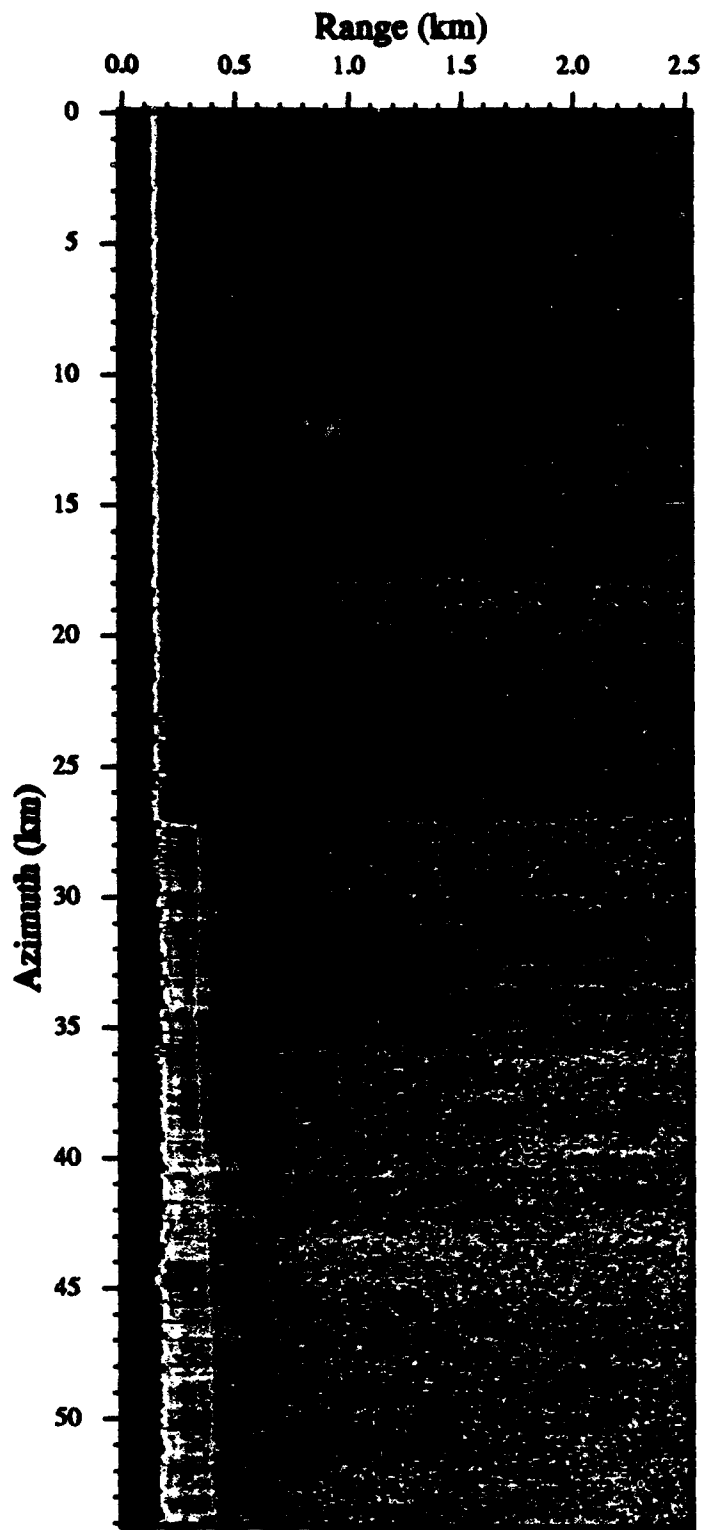


Figure 4.1-4c Ship Track D: Oceanic Mixed layer Measurements.
SST, Salinity, Current speed, Direction, And Shear at 8 m





RAR 19

	Start	End
Time:	16:06:32	16:15:25
Lat:	36.575°	36.043°
Lon:	74.217°	74.217°

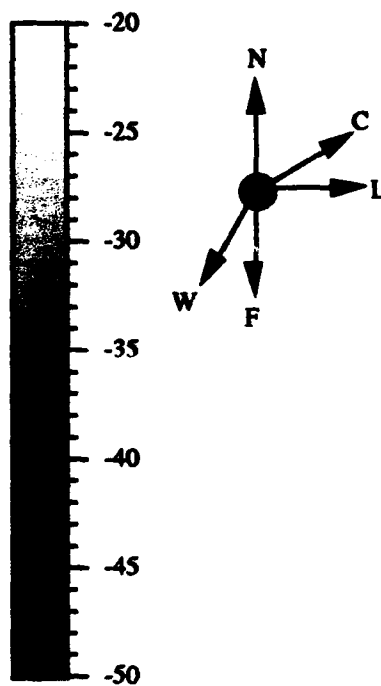
Flight Parameters

Heading:	180° T
Speed:	100 m s ⁻¹
Altitude:	174 m

RAR Parameters

Resolution (low)

Azimuth:	4 m
Range:	8 m
Polarization:	HH
Frequency:	9.375 GHz
Wave Length:	3 cm
Scan lines:	4847
Samples/scan:	404



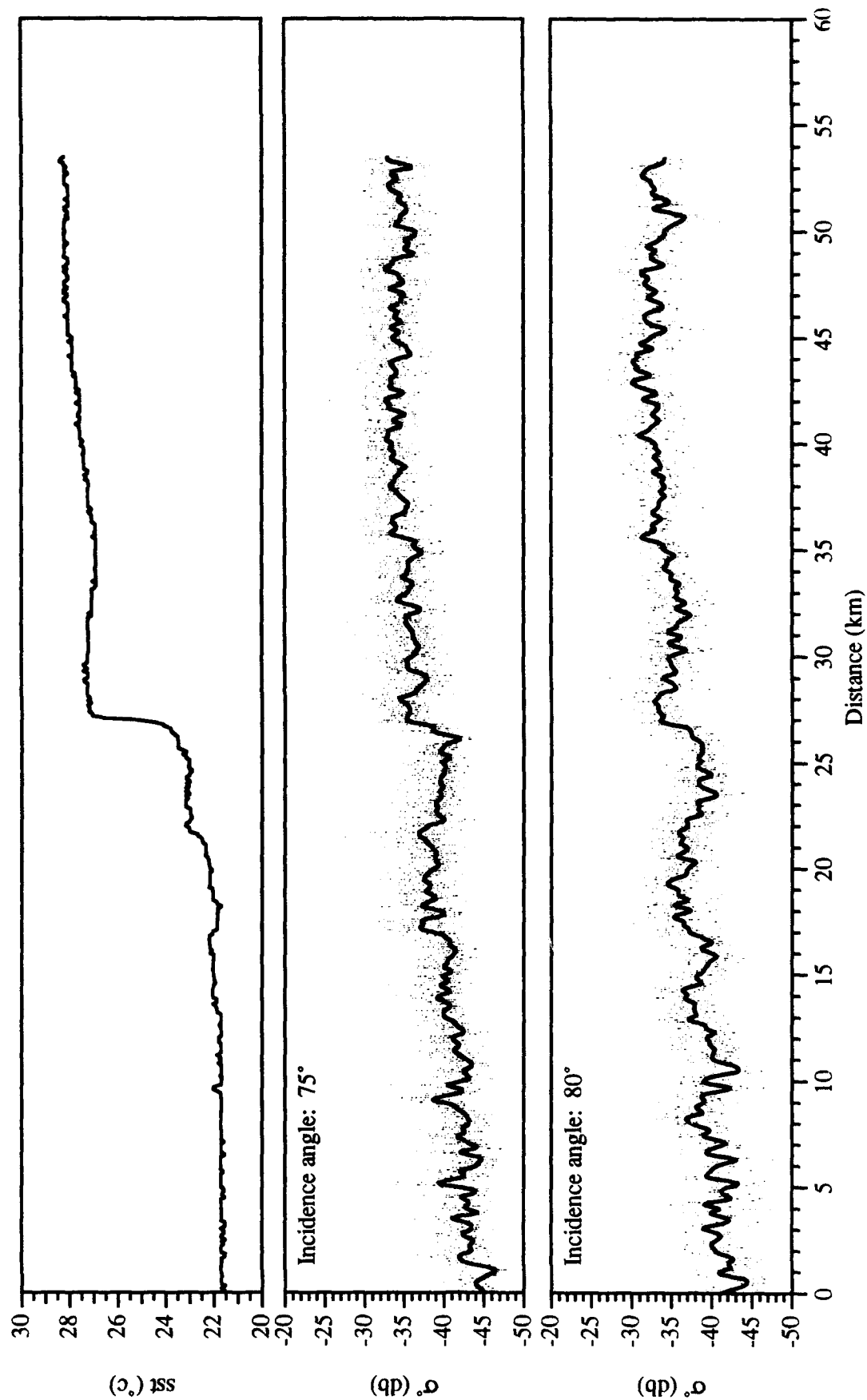
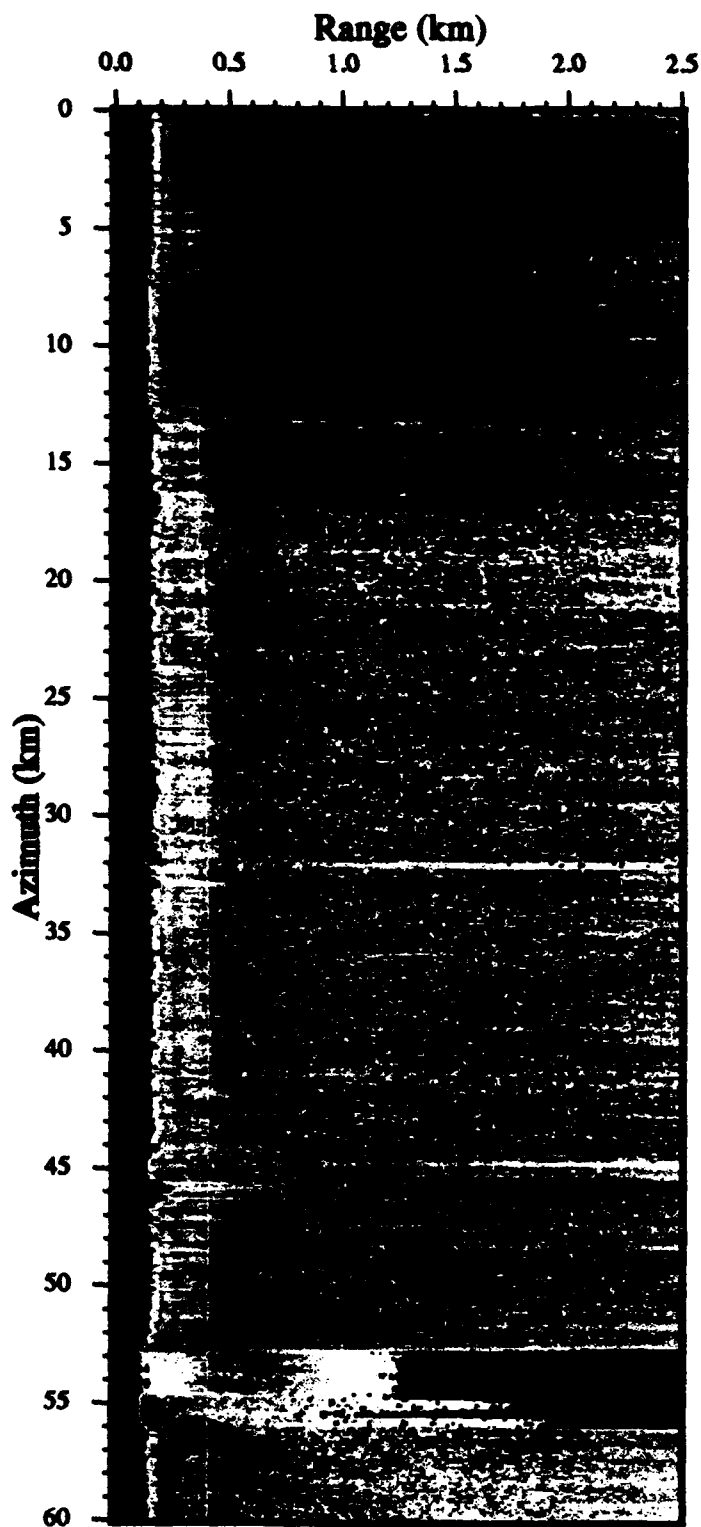


Figure xx.x RAR Track 19: SST and along track absolute cross section (σ') at 75 and 80°.



RAR 20

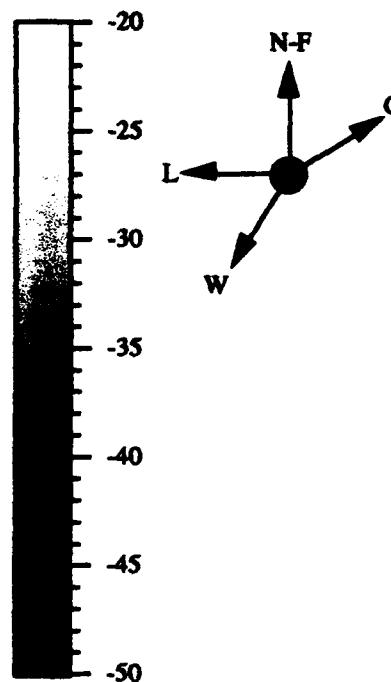
	Start	End
Time:	16:22:25	16:32:35
Lat:	35.988°	36.493°
Lon:	74.063°	74.063°

Flight Parameters

Heading:	0° T
Speed:	100 m s ⁻¹
Altitude:	174 m

RAR Parameters

Resolution (low)	
Azimuth:	4 m
Range:	8 m
Polarization:	HH
Frequency:	9.375 GHz
Wave Length:	3 cm
Scan lines:	5454
Samples/scan:	404



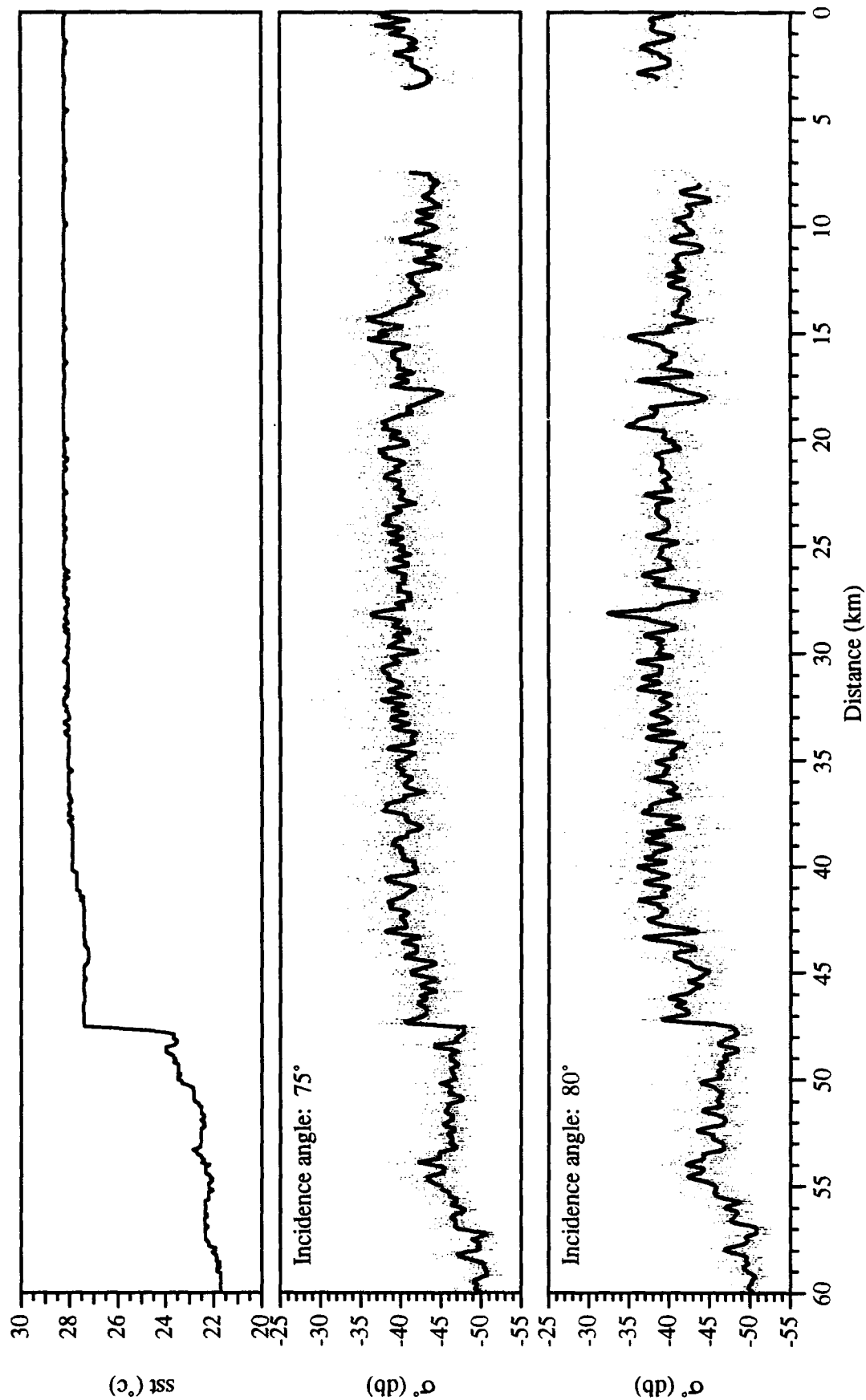
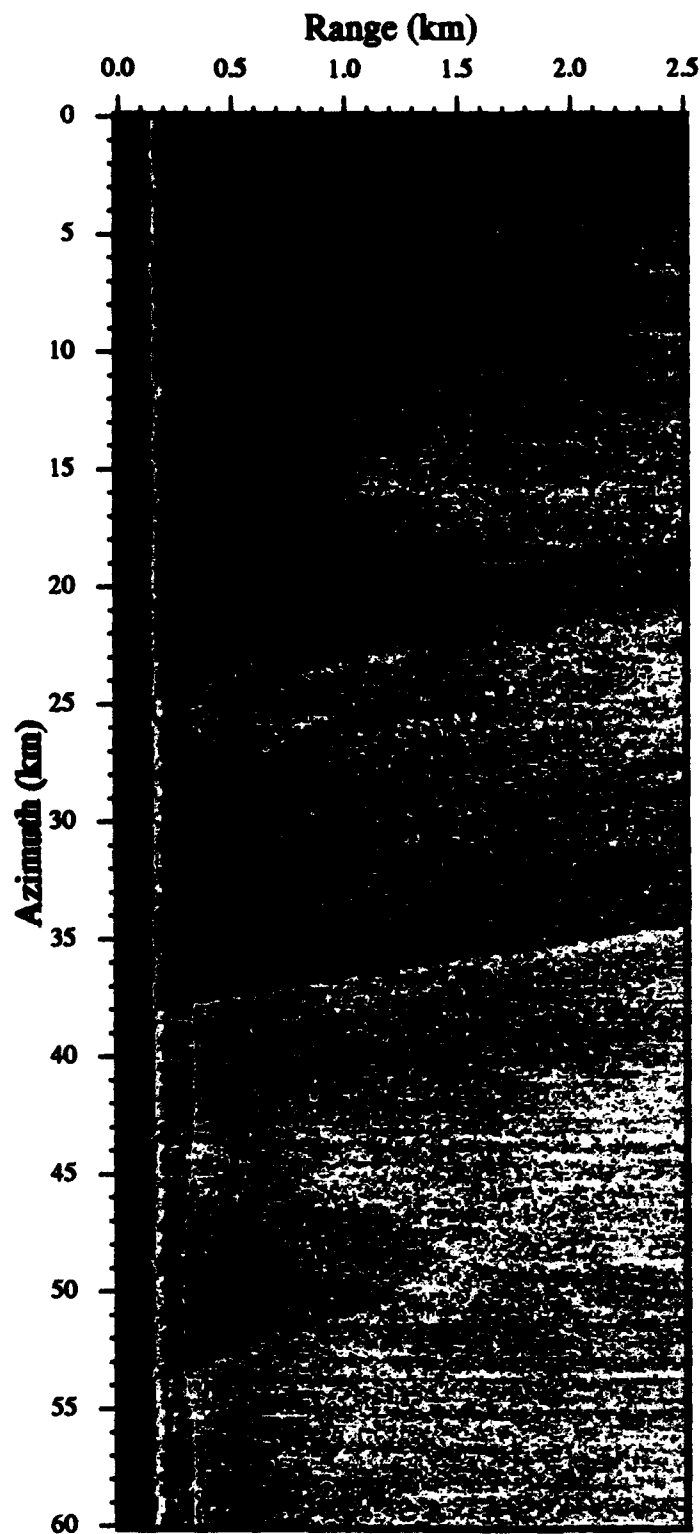


Figure xx.x RAR Track 20: SST and along track absolute cross sections (σ^0) at 75 and 80°.



RAR 22

	Start	End
Time:	16:45:08	16:55:07
Lat:	36.568°	36.160°
Lon:	73.887°	74.395°

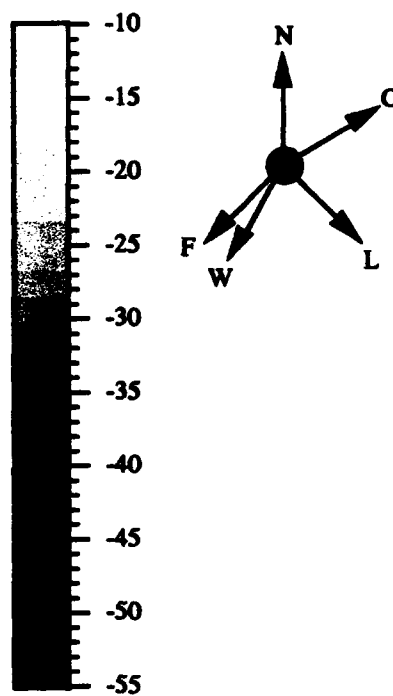
Flight Parameters

Heading:	225° T
Speed:	100 m s ⁻¹
Altitude:	174 m

RAR Parameters

Resolution (low)

Azimuth:	4 m
Range:	8 m
Polarization:	HH
Frequency:	9.375 GHz
Wave Length:	3 cm
Scan lines:	5454
Samples/scan:	404



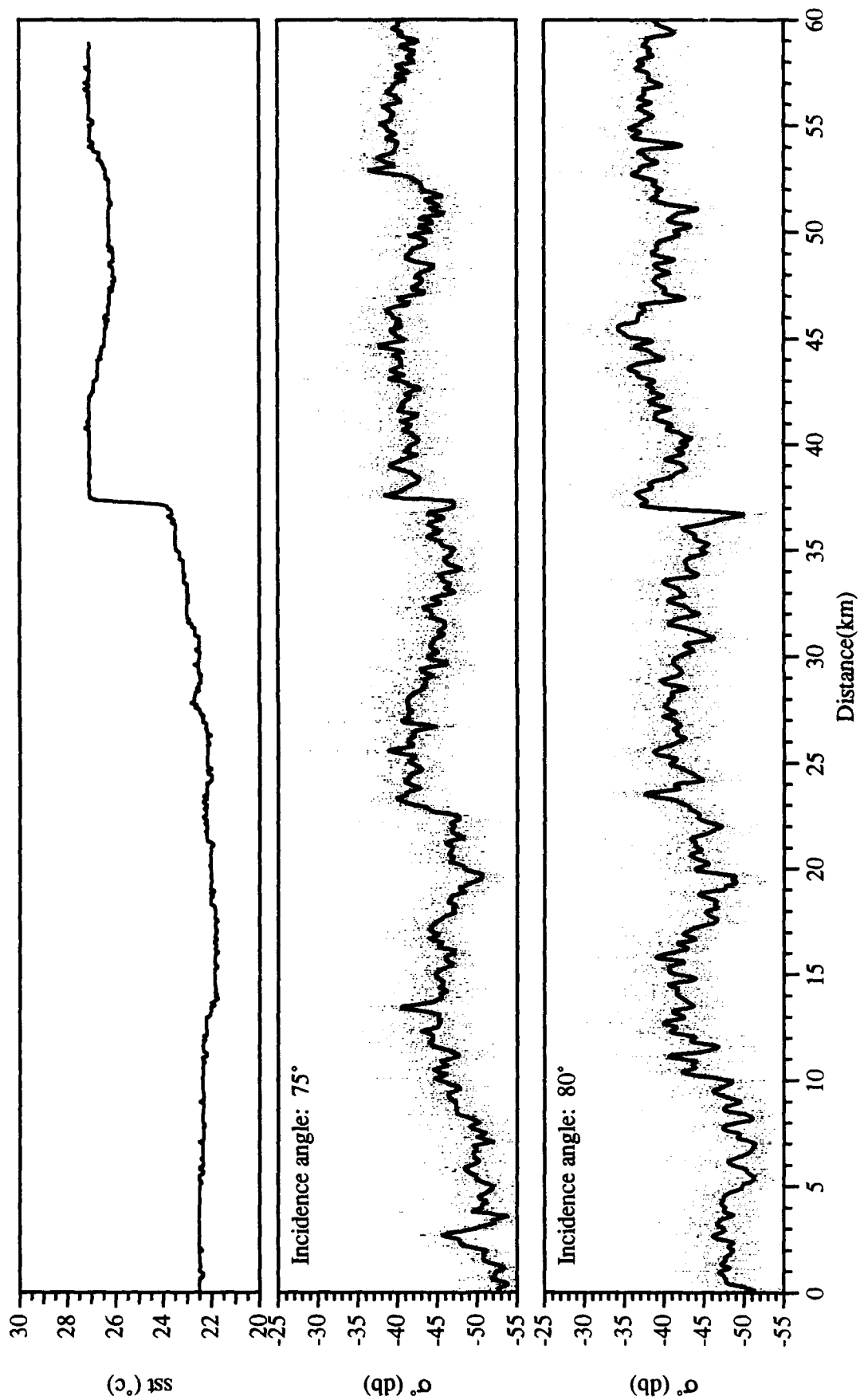
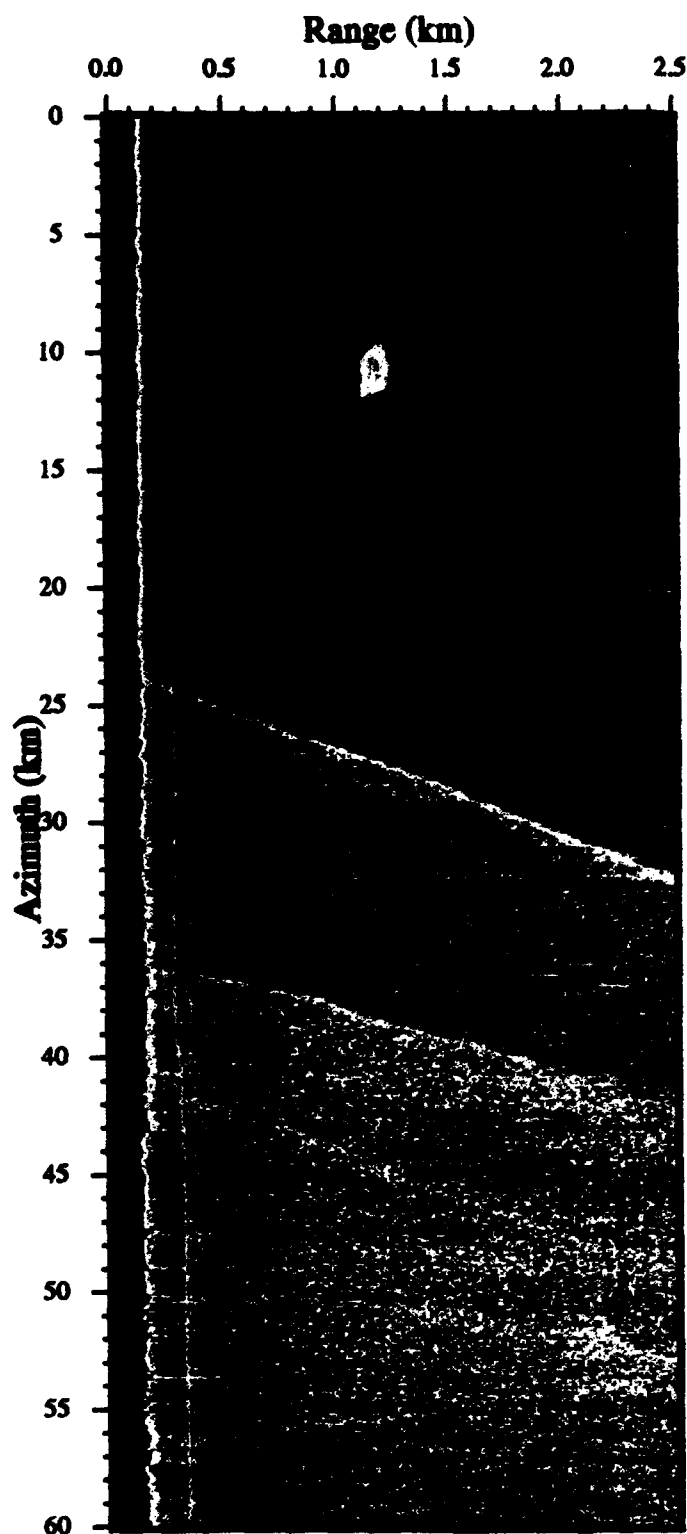


Figure xx.x RAR Track 22: SST and along track absolute cross section (σ^0) and at 75 and 80°.



RAR 23

	Start	End
Time:	17:04:46	17:14:45
Lat:	36.310°	36.310°
Lon:	74.448°	73.817°

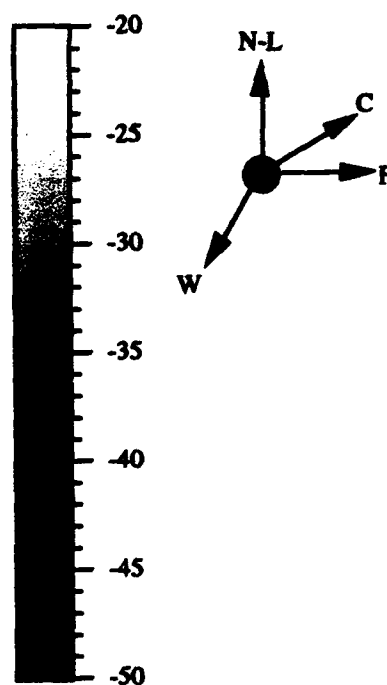
Flight Parameters

Heading:	90° T
Speed:	100 m s ⁻¹
Altitude:	174 m

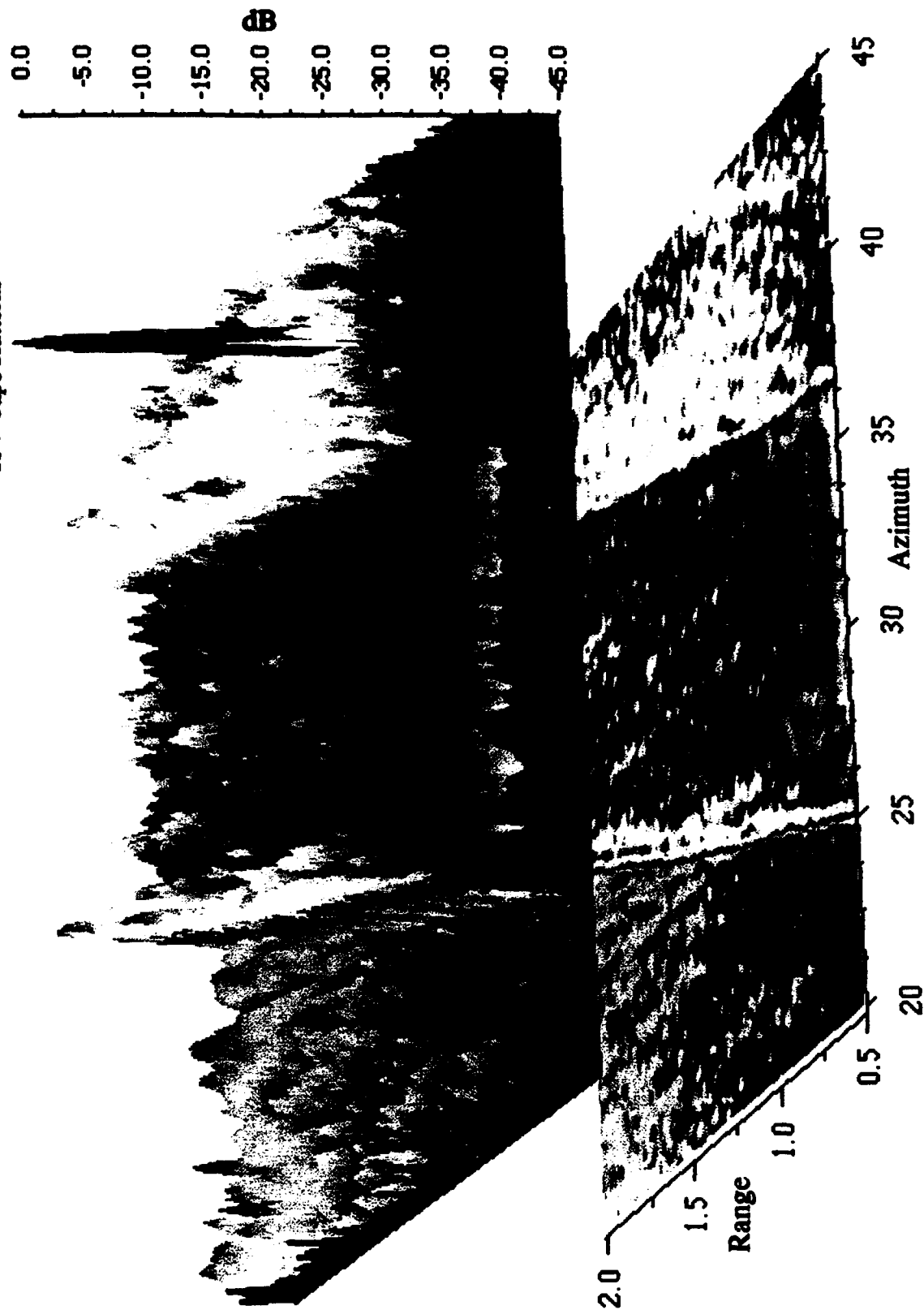
RAR Parameters

Resolution (low)

Azimuth:	4 m
Range:	8 m
Polarization:	HH
Frequency:	9.375 GHz
Wave Length:	3 cm
Scan lines:	5454
Samples/scan:	404



R/V Cape Hatteras



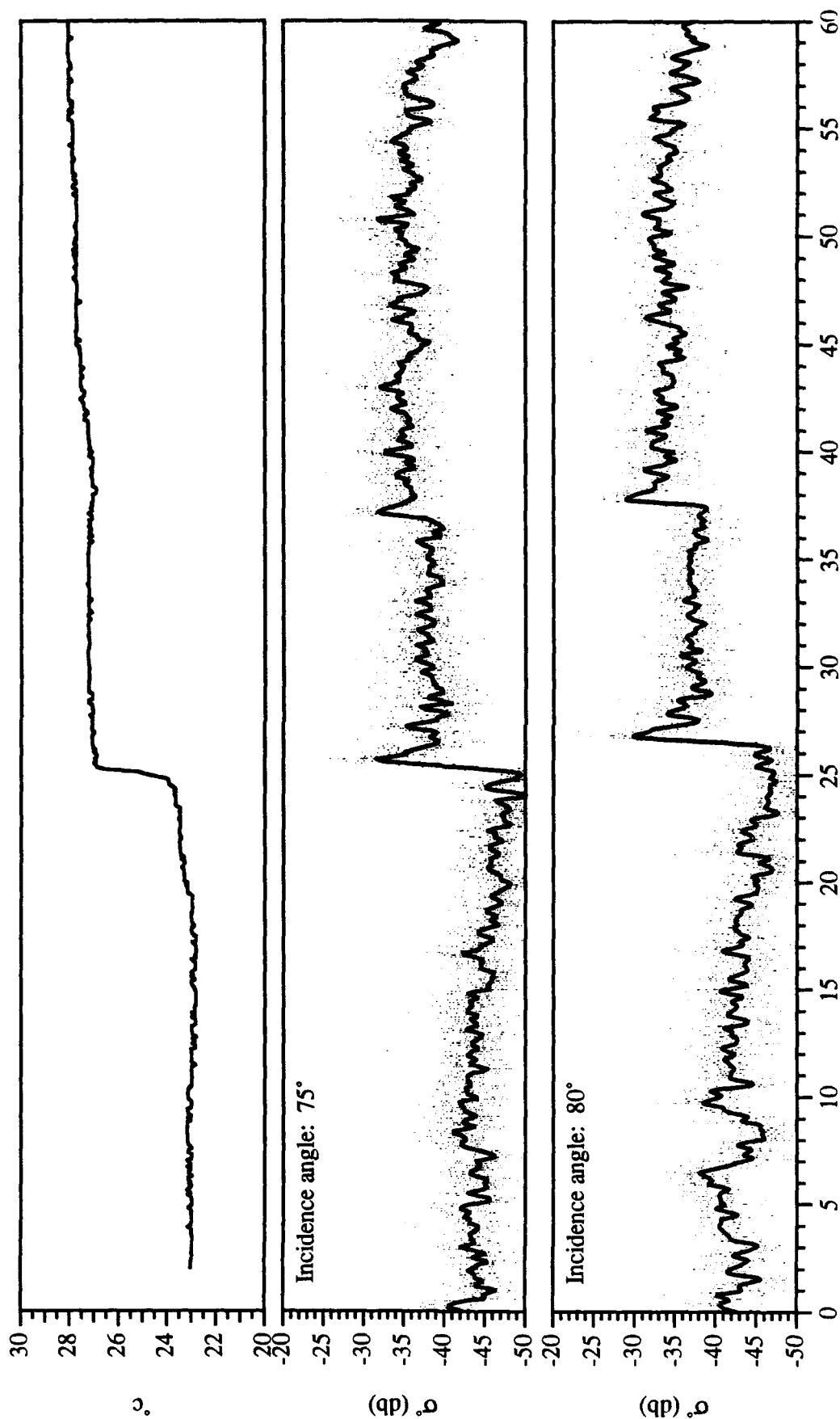
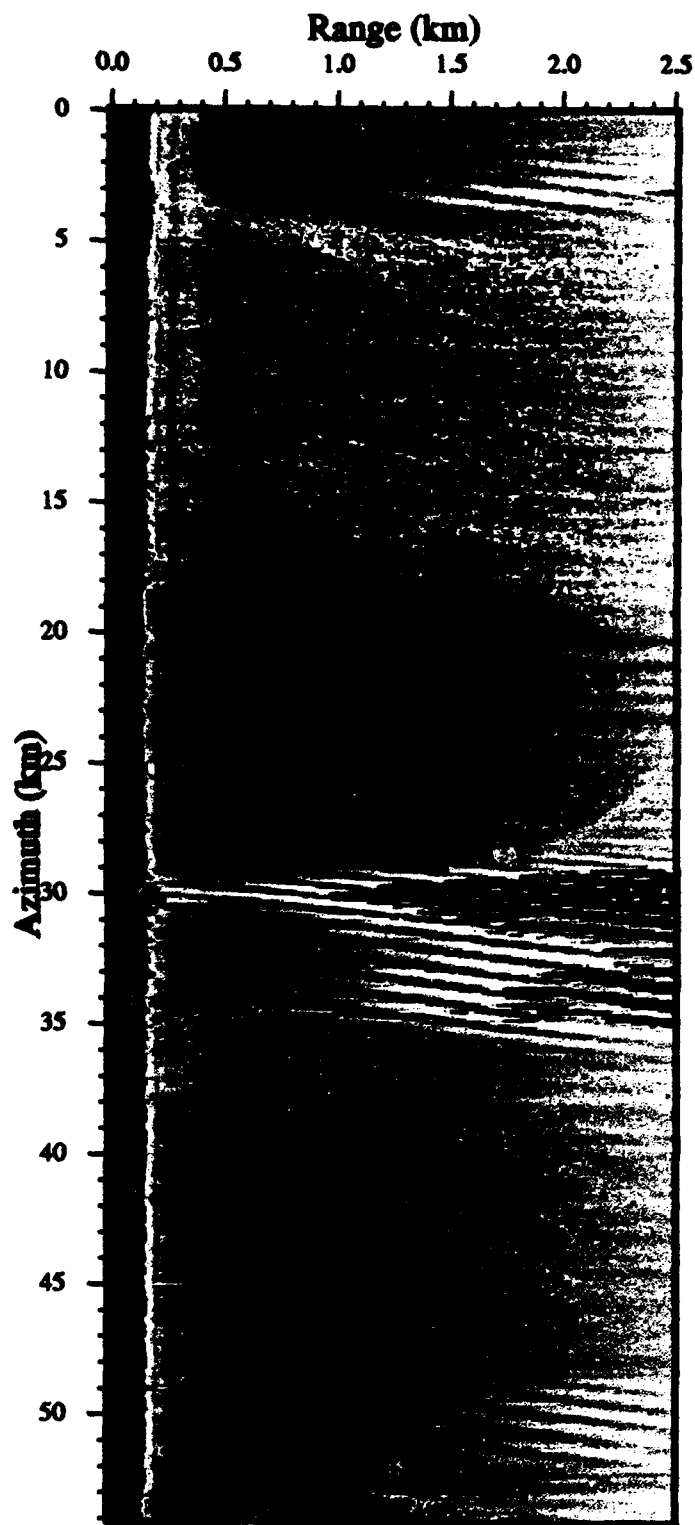


Figure xx.x RAR Track 23: SST and along track absolute cross section (σ^0) at 75 and 80°.



RAR 24

	Start	End
Time:	17:24:04	17:32:59
Lat:	36.438°	36.438°
Lon:	73.852°	74.512°

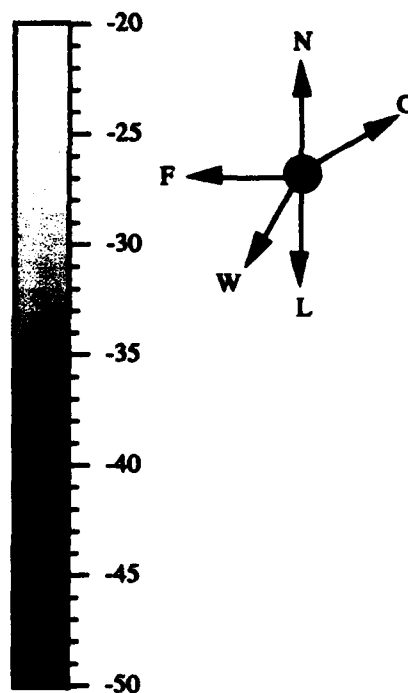
Flight Parameters

Heading:	270° T
Speed:	100 m s ⁻¹
Altitude:	174 m

RAR Parameters

Resolution (low)

Azimuth:	4 m
Range:	8 m
Polarization:	HH
Frequency:	9.375 GHz
Wave Length:	3 cm
Scan lines:	4869
Samples/scan:	404



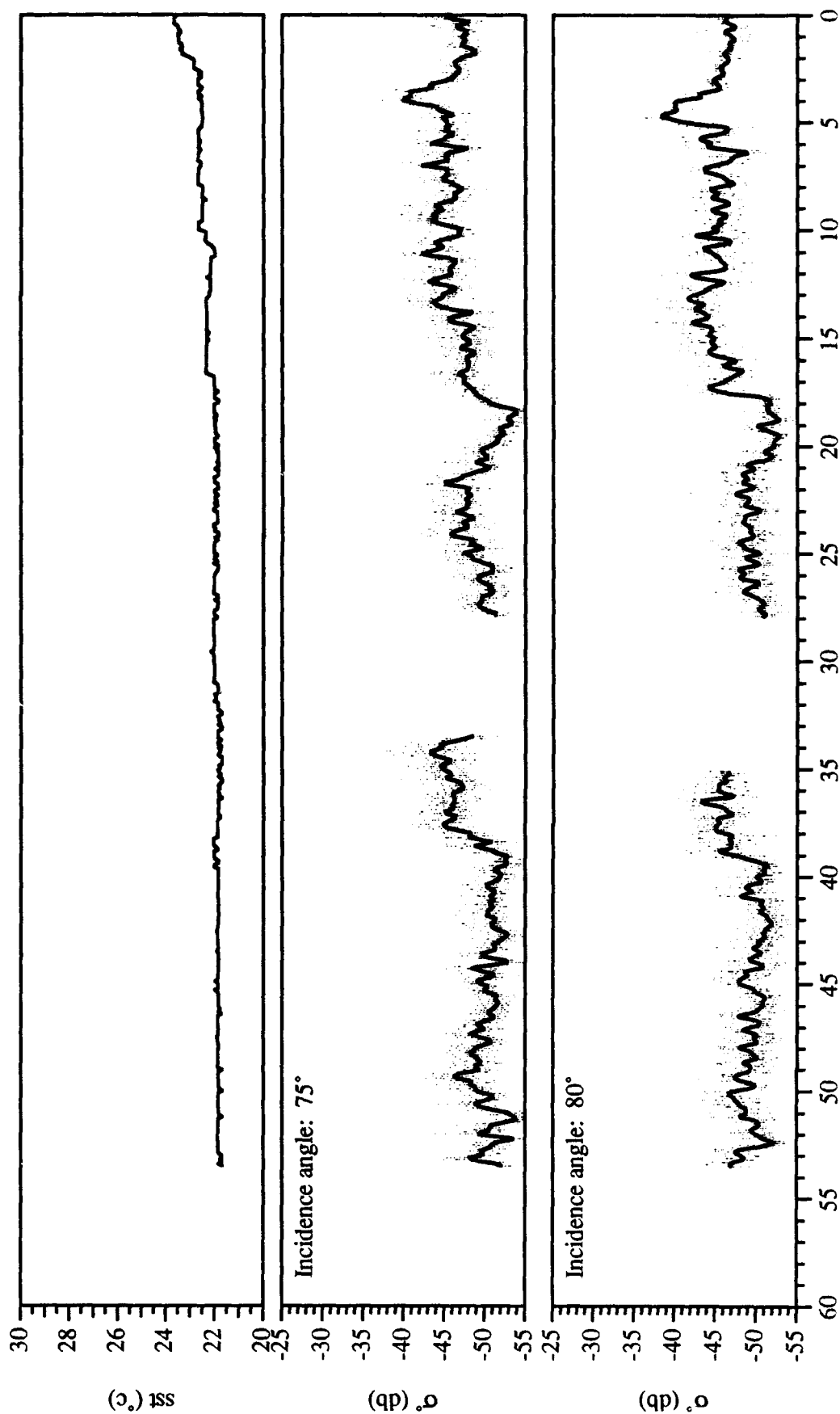
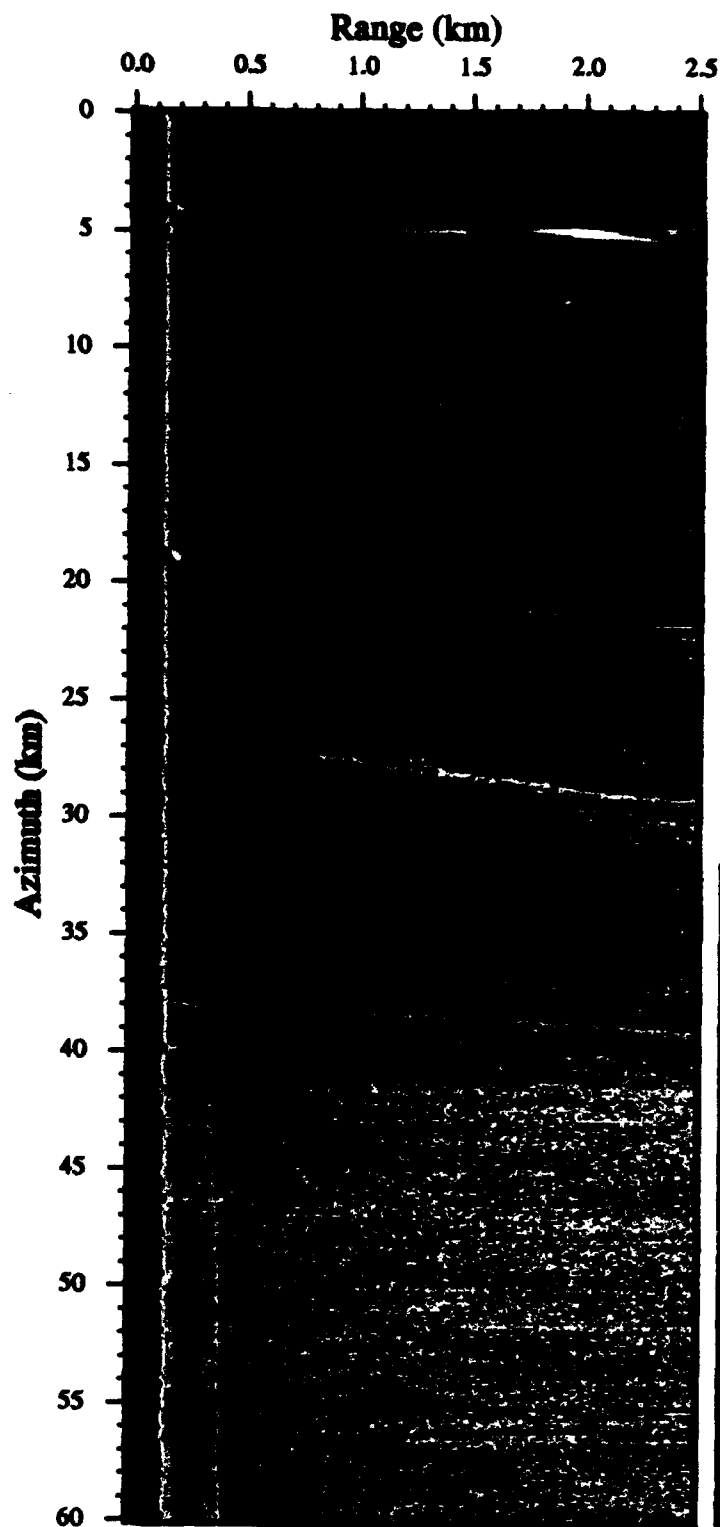


Figure xx.x RAR Track 24: SST and along track absolute cross section (σ') at 75 and 80°.



RAR 25

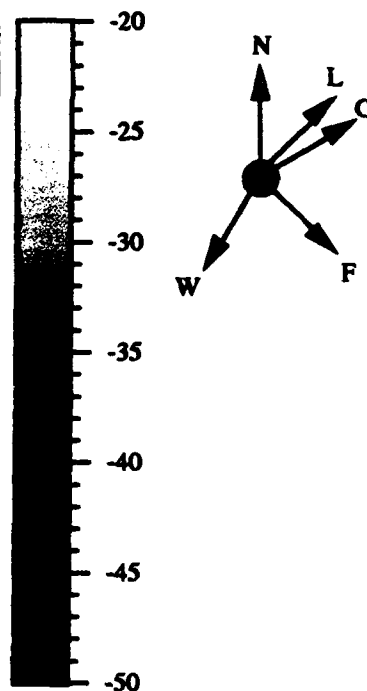
	Start	End
Time:	17:39:08	17:49:08
Lat:	36.543°	36.172°
Lon:	74.333°	73.935°

Flight Parameters

Heading:	136° T
Speed:	100 m s ⁻¹
Altitude:	174 m

RAR Parameters

Resolution (low)	
Azimuth:	4 m
Range:	8 m
Polarization:	HH
Frequency:	9.375 GHz
Wave Length:	3 cm
Scan lines:	5454
Samples/scan:	404



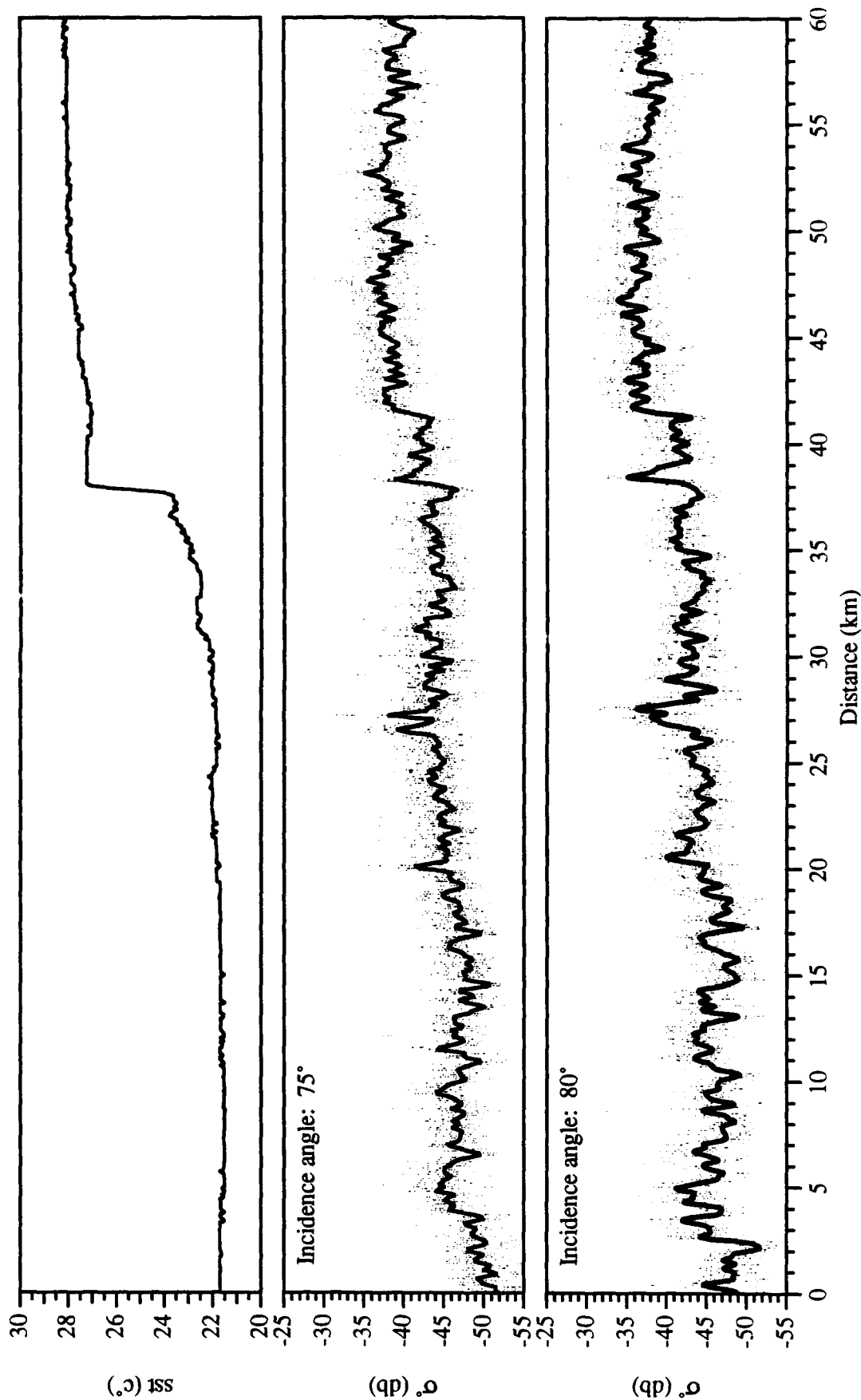


Figure xx.x RAR Track 25: SST and along track cross sections (σ°) at 75 and 80°.

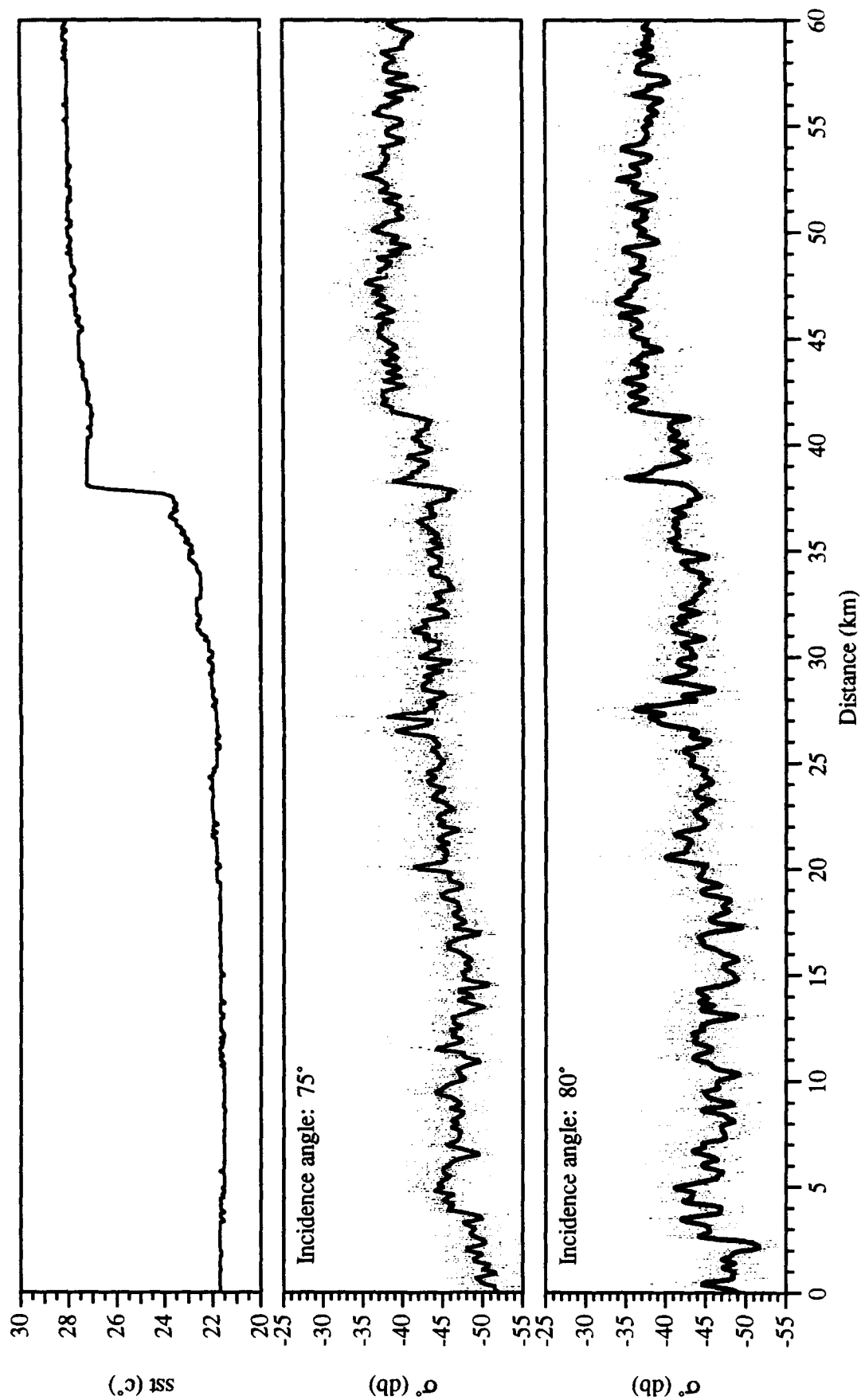
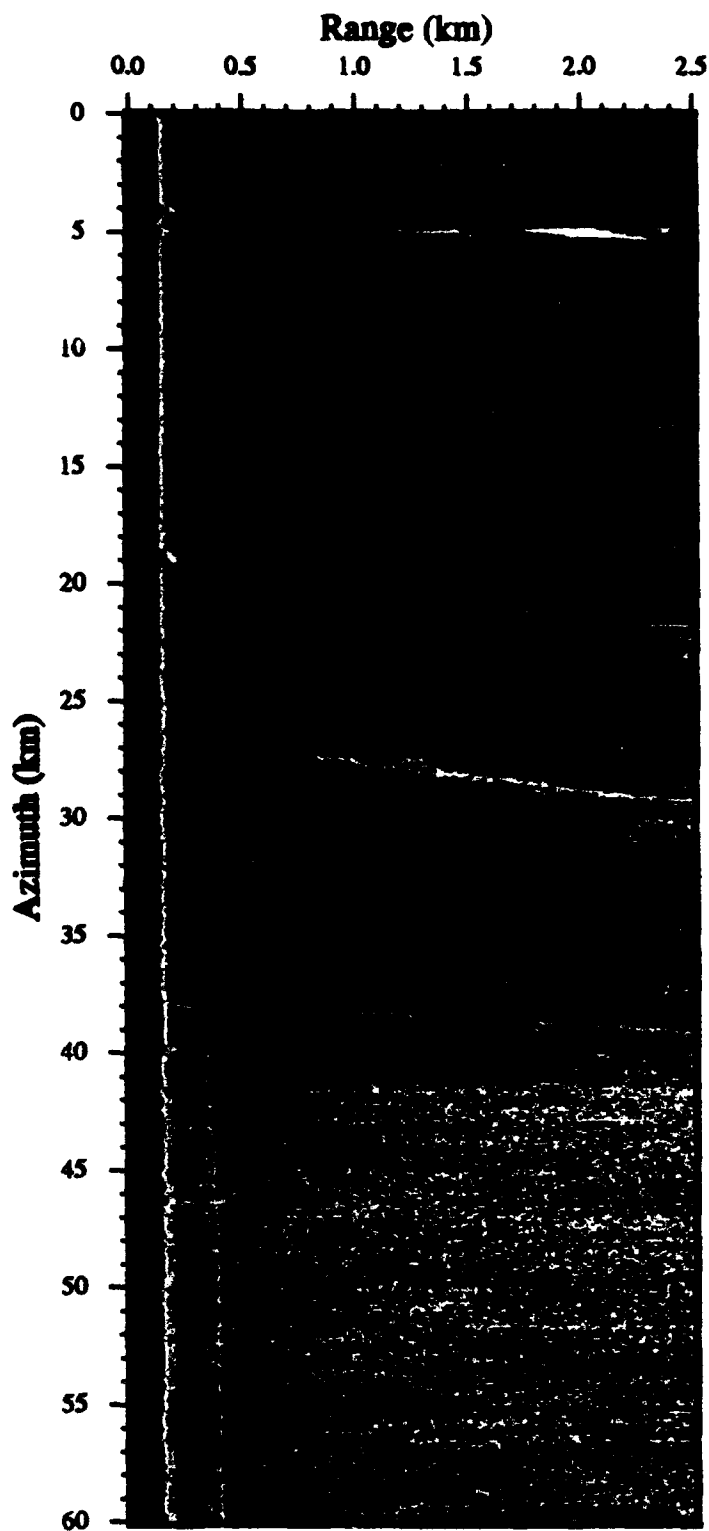


Figure xx.x RAR Track 25: SST and along track cross absolute cross sections (σ^0) at 75 and 80°.



RAR 25

	Start	End
Time:	17:39:08	17:49:08
Lat:	36.543°	36.172°
Lon:	74.333°	73.935°

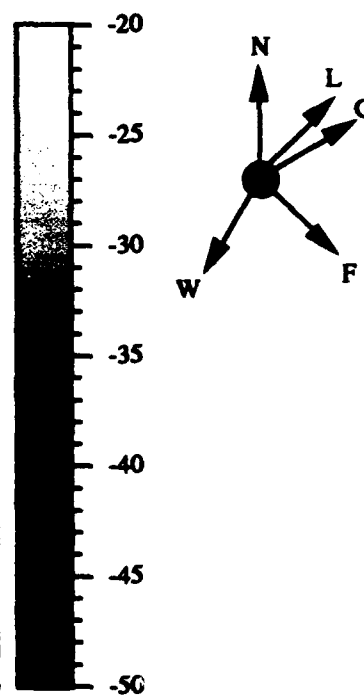
Flight Parameters

Heading:	136° T
Speed:	100 m s ⁻¹
Altitude:	174 m

RAR Parameters

Resolution (low)

Azimuth:	4 m
Range:	8 m
Polarization:	HH
Frequency:	9.375 GHz
Wave Length:	3 cm
Scan lines:	5454
Samples/scan:	404



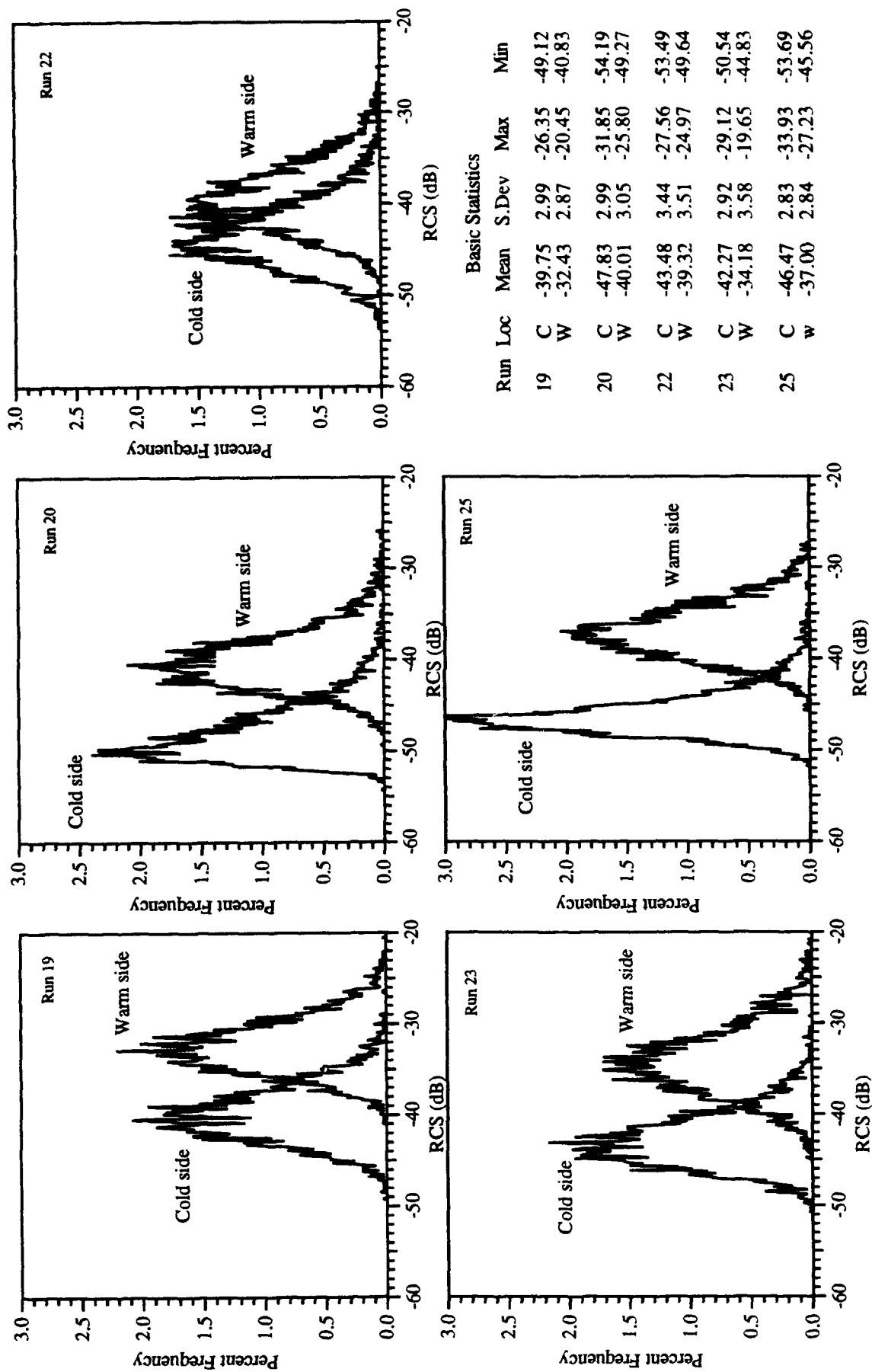


Figure XX.X Histograms and basic statistics for 64 X 64 squares on each side of the Gulf Stream SST Front